

THESIS FOR THE DEGREE OF DOCTOR OF PHILOSOPHY

# **Chemical-Looping Combustion with Liquid Fuel**

PATRICK MOLDENHAUER

Department of Energy and Environment  
CHALMERS UNIVERSITY OF TECHNOLOGY  
Gothenburg, Sweden 2014

Chemical-Looping Combustion with Liquid Fuel  
PATRICK MOLDENHAUER  
ISBN 978-91-7597-072-1

© PATRICK MOLDENHAUER, 2014

Doktorsavhandlingar vid Chalmers tekniska högskola  
Ny serie nr 3753  
ISSN 0346-718X

Department of Energy and Environment  
Chalmers University of Technology  
SE-412 96 Gothenburg  
Sweden  
Telephone +46 (0)31-772 1000

Cover:

The cover image shows the lower section of the fuel reactor with the injection system for liquid fuels. This section is part of the pilot-scale chemical-looping reactor and was designed as part of this thesis.

Chalmers Reproservice  
Gothenburg, Sweden, 2014

## Abstract

Chemical-looping combustion (CLC) is a promising technology for future energy conversion on the basis of combustion of fossil fuels with inherent CO<sub>2</sub> separation. In comparison to other carbon-capture technologies there is no need for energy demanding gas separation in order to obtain pure CO<sub>2</sub>. In the past, CLC research has mainly focused on the use of gaseous and solid fuels. This work the first comprehensive study of the use of liquid fuels in chemical-looping combustion. The work in the thesis includes (1) investigation of several different oxygen carriers based on nickel, iron, manganese and copper with kerosene as fuel, (2) design of an injection system for heavy liquid fuels for the fuel reactor of a pilot-scale chemical-looping reactor, (3) long-term operation of ilmenite oxygen carrier with a fuel oil in a pilot-scale unit and (4) tests with ilmenite oxygen carrier and a vacuum residue from Saudia Arabia as fuel.

Experiments were conducted in a bench-scale reactor and in a pilot-scale reactor, and for each reactor a fuel injection system was designed and tested. Two types of kerosene, with and without sulphur, were tested in the bench-scale reactor during 240 h of fuel injection and a fuel input between 100 W<sub>th</sub> and 580 W<sub>th</sub>. In the pilot-scale system, a fuel oil type 1 and different blends of a vacuum residue and fuel oil 1 were tested during 72 h of fuel operation. Here, the fuel input was varied between 4.5 kW<sub>th</sub> and about 6 kW<sub>th</sub>.

Six different oxygen-carrier materials, out of which four were synthesized and two were of mineral origin, were tested in the bench-scale unit. The different materials showed clear differences in fuel conversion and structural integrity. Ilmenite oxygen carrier, which is a mineral iron–titanium oxide, was found to have a high structural stability, which was unmatched by the synthesized materials. Fuel conversion, however, was significantly lower than that of the synthesized oxygen carriers, and it is likely that temperatures above 950°C are needed in order to achieve reasonable conversion levels.

Long-term testing was carried out with the ilmenite oxygen carried in the pilot-scale reactor system. The conditions in this unit are much harsher than those in the bench-scale reactor and similar to those in an industrial-scale circulating fluidized-bed boiler. With fuel oil 1 as fuel, different trends in fuel conversion could be observed with respect to reactor temperature, fuel flow and solids circulation. After modifying the fuel injection system, two different blends of vacuum residue and fuel oil were injected. At most, 80 wt% vacuum residue was blended with 20 wt% fuel oil. It was found that the conversion of the different blends tested did not deviate significantly from the conversion of unblended fuel oil. The total fuel operation time in the pilot-scale unit was about 72 h and the ilmenite particles were fluidized at high temperatures for more than 340 h without any significant problems concerning agglomeration or disintegration.



---

# Acknowledgements

---

I would very much like to thank my supervisors Tobias Mattisson and Magnus Rydén and my examiner Anders Lyngfelt. You introduced me to the field of chemical-looping, listened patiently to my questions, always had open doors and ears for discussion and – very important! – signed the invoices for all the stuff I bought. I couldn't have asked for better supervisors. Thanks for you three for everything!

A big thanks to my fellow loopers for the good group spirit, fruitful discussions and shared agony in the lab. Thank you, in no particular order, Strong Peter, Mr. CLC3 Calle, Glicksman Pontus, Erik Jerndeiro, Marching-Band Henrik, Lab-Order Golnar, Speedy Gon-Mehdi, Dazinho, Nippon Martin, Fleisch-ist-mein-Gemüse Matthias, Jack-of-all-Trades Georg, SEM Pavletta, Partyhouse Dongmei, Sledgehammer Sebbe, Particle-Alchemist Nasim, Graphics Miracle-Worker Jesper, Lab-Enthusiast Malin, Velcrosuit Volkmar and our two Fulbrighters, Chuck and Azad.

Not all the help I received came from within the chemical-looping group. Helping hands and ideas came from all around: Martin Seemann, Fredrik Lind, Nicolas Berguerand, Sven-Ingvar Andersson, David Pallarès, Filip Johnsson, Sven Andersson, Roger Sagdahl, Lars-Erik Åmand, Mikael Israelsson and Jessica Bohwalli. Tack, tack, tack! A special thanks to Ulf and Rustan for countless occasions of enthusiastic tech-talk and lots of technical help.

Thanks also to the participants of the board game nights and the soccer matches at Energy Technology. Your spirit was highly appreciated!

One big collective thank you to the rest of my co-workers at the division of Energy Technology for the nice working atmosphere: the systematics, the burners (formerly known as the oxycrowd), the administratives(!), the life cyclers, the fluidizers, the gas people and everybody else, who feels at home at Energy Technology!

This project, “Chemical-looping with liquid hydrocarbon fuels”, wouldn't have been on its way without Saudi Aramco's belief in chemical looping and their will to invest money in it. I want to thank Jean-Pierre Ballaguet, Bandar Fadhel, Wajdi Sadat, Tidjani Niass, Mourad Younes, Aqil Jamal and Ali Hoteit from Saudi Aramco for the friendly cooperation.

Long hours in the lab and in the office, worries about deadlines and too many different different things in my head. Family and friends helped me to keep a healthy balance. Thanks to my Friends Anton, Érika and Daniel. Karin, you lifted me up on countless

---

occasion with all your small shenanigans and your bright smiles and laughter. The last sentences of my acknowledgements are for you Karolina: Without all your support and affection, life wouldn't have been nearly as exciting, bright and fantastic. I love you and I'm grateful for all your support!

*Patrick Moldenhauer*  
*Gothenburg, September 2014*

---

# List of Publications

---

This thesis is based on the following publications:

- I. P. Moldenhauer, M. Rydén, and A. Lyngfelt. Testing of minerals and industrial by-products as oxygen carriers for chemical-looping combustion in a circulating fluidized-bed 300 W laboratory reactor. *Fuel*, 93:351–363, 2012
- II. P. Moldenhauer, M. Rydén, T. Mattisson, and A. Lyngfelt. Chemical-looping combustion and chemical-looping reforming of kerosene in a circulating fluidized-bed 300 W laboratory reactor. *International Journal of Greenhouse Gas Control*, 9:1–9, 2012
- III. P. Moldenhauer, M. Rydén, T. Mattisson, and A. Lyngfelt. Chemical-looping combustion and chemical-looping with oxygen uncoupling of kerosene with Mn- and Cu-based oxygen carriers in a circulating fluidized-bed 300 W laboratory reactor. *Fuel Processing Technology*, 104:378–389, 2012
- IV. P. Moldenhauer, M. Rydén, T. Mattisson, M. Younes, and A. Lyngfelt. The use of ilmenite as oxygen carrier with kerosene in a 300 W CLC laboratory reactor with continuous circulation. *Applied Energy*, 113:1846–1854, 2014
- V. P. Moldenhauer, M. Rydén, T. Mattisson, A. Hoteit, A. Jamal, and A. Lyngfelt. Chemical-Looping Combustion with Fuel Oil in a 10 kW Pilot Plant. *Energy & Fuels*, 28(9):5978–5987, 2014

## Contribution report

- Papers I, II and IV: Principal author, responsible for the majority of the experimental work and data evaluation.
- Papers III and V: Principal author, responsible for all experimental work and data evaluation.

---

Other related publications and contributions that are not included in this thesis:

- P. Moldenhauer, M. Rydén, T. Mattisson, M. Younes, and A. Lyngfelt. The use of ilmenite as oxygen carrier with kerosene in a 300 W CLC laboratory reactor with continuous circulation. In *Proceedings of the 2<sup>nd</sup> International Conference on Chemical Looping*, Darmstadt, Germany, 2012<sup>†</sup>
- M. Rydén, P. Moldenhauer, T. Mattisson, A. Lyngfelt, M. Younes, T. Niass, B. Fadhel, and J.-P. Ballaguet. Chemical-Looping Combustion with Liquid Fuels. *Energy Procedia*, 37:654–661, 2013<sup>‡</sup>
- T. Mattisson, P. Moldenhauer, A. Hoteit, M. Rydén, A. Jamal, and A. Lyngfelt. Chemical-looping combustion of liquid hydrocarbon fuels. In *Proceedings of the 3<sup>rd</sup> International Conference on Chemical Looping*, Gothenburg, Sweden, 2014<sup>§</sup>
- M. Rydén, P. Moldenhauer, S. Lindqvist, T. Mattisson, and A. Lyngfelt. Measuring attrition resistance of oxygen carrier particles for chemical looping combustion with a customized jet cup. *Powder Technology*, 256:75–86, 2014
- M. Rydén, P. Moldenhauer, T. Mattisson, and A. Lyngfelt. Attrition of oxygen carrier particles in fluidized bed – basic theory and screening measurements with a customized jet cup test rig. In *Proceedings of the 3<sup>rd</sup> International Conference on Chemical Looping*, Gothenburg, Sweden, 2014<sup>§</sup>

<sup>†</sup> This work was also presented as a poster at the 2<sup>nd</sup> International Conference on Chemical looping in Darmstadt, Germany, 26-28 September, 2012.

<sup>‡</sup> This work was also presented as a poster at the 11<sup>th</sup> International Conference on Greenhouse Gas Control Technologies in Kyoto, Japan, 18-22 November, 2012.

<sup>§</sup> This work was also presented orally at the 3<sup>rd</sup> International Conference on Chemical looping in Gothenburg, Sweden, 9-11 September, 2014.

---

# Contents

---

<b>1</b>	<b>Introduction</b>	<b>1</b>
1.1	Chemical-Looping Combustion . . . . .	2
1.1.1	Chemical-Looping with Oxygen Uncoupling . . . . .	3
1.1.2	Chemical-Looping Reforming . . . . .	4
1.1.3	Chemical-Looping Combustion with Liquid Fuel . . . . .	5
1.2	Aim and Scope . . . . .	9
1.3	Content of the Thesis . . . . .	9
<b>2</b>	<b>Experimental Details</b>	<b>13</b>
2.1	Chemical-Looping Reactors . . . . .	13
2.1.1	Bench-Scale Reactor . . . . .	13
2.1.2	Pilot-Scale Reactor . . . . .	15
2.2	Liquid Fuels . . . . .	16
2.2.1	Kerosene . . . . .	16
2.2.2	Fuel Oil . . . . .	19
2.2.3	Vacuum Residue . . . . .	19
2.3	Injection Systems for Liquid Fuel . . . . .	20
2.3.1	Fuel Vaporization Concept . . . . .	20
2.3.2	Direct Injection Concept . . . . .	21
2.4	Measurements . . . . .	23
2.5	Oxygen Carriers . . . . .	24
2.5.1	Particle Preparation . . . . .	24
2.5.2	Synthetic Nickel-based Material . . . . .	26
2.5.3	Mineral Ilmenite Material . . . . .	26
2.5.4	Synthetic Manganese-based Material . . . . .	27
2.5.5	Synthetic Copper-based Materials . . . . .	27
2.5.6	Manganese Ore . . . . .	28
2.5.7	Synthetic Calcium Manganite-based Material . . . . .	28
2.6	Experiments Performed . . . . .	28
2.6.1	Syngas Experiments . . . . .	28
2.6.2	Kerosene Experiments . . . . .	29
2.6.3	Fuel Oil Experiments . . . . .	31
2.6.4	Vacuum Residue Experiments . . . . .	32

<b>3</b>	<b>Results and Discussion</b>	<b>35</b>
3.1	Syngas Experiments . . . . .	35
3.2	Kerosene Experiments . . . . .	35
3.2.1	Sulphur-free Kerosene . . . . .	35
3.2.2	Sulphurous Kerosene . . . . .	40
3.3	Fuel Oil Experiments . . . . .	42
3.4	Vacuum Residue Experiments . . . . .	48
3.4.1	Improvements of the Injection System for Vacuum Residue . . . . .	50
<b>4</b>	<b>Conclusions</b>	<b>53</b>
	<b>Nomenclature</b>	<b>55</b>
	<b>Bibliography</b>	<b>57</b>





---

# 1 Introduction

---

Carbon dioxide that is emitted into the atmosphere has the potential to change the climate of the Earth. This has been known for at least 100 years [1]. Initially, such a climate change was seen as a way to attenuate ice ages. Later, as knowledge grew, the dangers of such a global climate change were understood. For more than 100 years, the concentrations of greenhouse gases in the atmosphere have been rising towards levels, where serious consequences for the climate of the Earth are expected [2, 3]. The Kyoto Protocol was a first agreement of nations on the common strategy of reducing greenhouse gas emissions [4]. Even though the so-called industrialized countries, i.e. countries defined as Annex I countries in the Kyoto Protocol including the United States and Canada, have met their collective target of reducing greenhouse gas emissions by 4.2% on average [5], the global emission of greenhouse gases continues to rise and no effective global successor for the Kyoto Protocol has yet been agreed upon.

There is general scientific agreement that the increase in anthropogenic greenhouse gas concentrations in the atmosphere is the main cause for the rise in global average temperatures, which have been observed since the mid-twentieth century. Further, during the 2010 United Nations Climate Change Conference, it was agreed that this so-called global warming should be limited to 2°C [6]. Since the rise in the average temperature on the surface of the Earth depends on the concentration of greenhouse gases in the atmosphere, it can be estimated how much more greenhouse gases, i.e. mostly carbon dioxide, can be emitted in order to stay below the 2°C-limit. Unfortunately, the carbon bound in the global fossil-fuel reserves exceeds this global carbon budget clearly, which means that severe consequences are likely to occur if humanity does not constrain and eventually stop the emission of greenhouse gases, especially CO<sub>2</sub> [7]. Also, the longer the time period is before greenhouse gas emissions are cut, the more drastic and rapid the measures will have to be that curtail emissions. This implies that the transient cost will be high [8]. An immediately initiated transient towards the goal of reaching an atmospheric concentration of about 450 ppm CO<sub>2</sub>-equivalent by 2100, would reduce the annualized consumption growth by about 0.06%-points of the average yearly growth anticipated for this century [9].

One possibility to reduce CO<sub>2</sub> emissions for the combustion of carbon-based fuels is through carbon capture and storage (CCS). In CCS, CO<sub>2</sub> is captured, transported and stored in underground storage locations [10]. One approach is to capture CO<sub>2</sub> at the combustion site, e.g. from fossil-fuel power plants, via either post-combustion CO<sub>2</sub> capture or oxyfuel combustion, e.g. chemical-looping combustion. Alternatively, carbon-based fuel is reformed

into a carbon-free fuel, i.e. hydrogen, and  $\text{CO}_2$  is captured before the actual fuel is used. This is commonly referred to as pre-combustion capture.

## 1.1 Chemical-Looping Combustion

Chemical-looping combustion (CLC) is a combustion process with inherent separation of  $\text{CO}_2$ . Combustion air and fuel are never mixed and, therefore, the flue gases are not diluted with nitrogen. Instead, the oxygen in the combustion air reacts with a solid oxygen carrier, which is then transported to the fuel. During a flameless oxidation, the oxygen leaves the oxygen carrier and reacts with the fuel, ideally forming  $\text{H}_2\text{O}$  and  $\text{CO}_2$ . A flue gas stream of pure  $\text{CO}_2$  can be obtained after condensing the steam in the flue gas. In chemical-looping combustion, the net heat of reaction is the same as in a normal combustion, i.e. with air. Therefore, a direct energy penalty for the separation of  $\text{CO}_2$ , which many other carbon-capture technologies suffer from, can be avoided.

In the most commonly proposed way of implementing chemical-looping combustion, oxygen-carrier particles are continuously circulated between two interconnected fluidized-bed reactors, the air reactor and the fuel reactor. The two reactors are connected through loop seals, which allow the fluidized oxygen carrier to pass from one reactor to the other but suppress gas leakage between the two reactors. In the air reactor, the oxygen carrier is oxidized with the combustion air. Thereafter, it is transported to the fuel reactor, where it is reduced by the fuel, which, in turn, is oxidized. This continuous cycle is illustrated in Figure 1.1. The basic reactions in the air reactor and the fuel reactor are expressed by Reactions (R1) and (R2), respectively. Here,  $\text{Me}_x\text{O}_y$  denotes a metal oxide, i.e. the oxygen carrier. The oxidation of the oxygen carrier in the air reactor is exothermic, whereas the reduction reaction in the fuel reactor can be either exothermic or endothermic, depending on the oxygen-carrier material and fuel used.

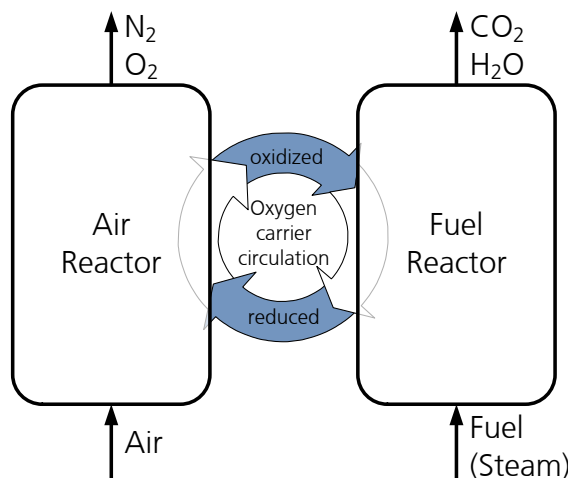
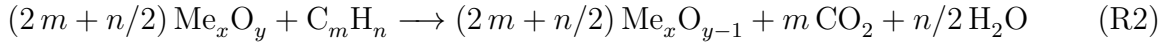
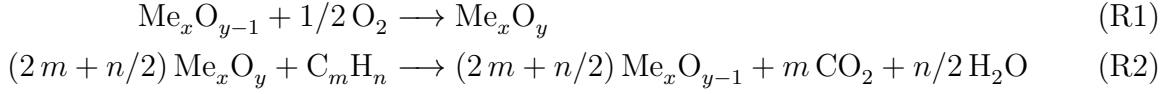


**Figure 1.1:** Schematic illustration of the chemical-looping combustion process

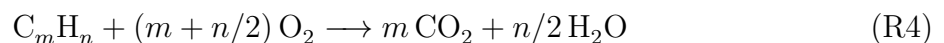
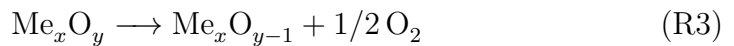


The first chemical-looping combustion experiments were published in 1951 by Lewis et al., who tested an iron ore and a synthesized copper-based oxygen carrier in a batch fluidized-bed reactor with metallurgical coke as fuel [11]. More than 40 years later, in 1994, Ishida and Hongguang established the term “chemical-looping combustion” and published experiments conducted in a thermogravimetric analyzer with hydrogen as fuel and different oxygen-carrier materials based on nickel and iron [12]. In 2003, the first successful continuous experiments with natural gas as fuel were performed by Lyngfelt and Thunman, and published in 2005 [13]. Operational experience of continuous chemical-looping combustion with solid fuels was first reported in 2008 by Berguerand and Lyngfelt [14]. The first continuous chemical-looping combustion experiments with liquid fuel are part of this thesis and were performed in 2010, see Paper II [15].

Recent literature concerning developments, advancements and operational experience in chemical-looping has been published by Fan [16], Adánez et al. [17] and Lyngfelt [18]. In 2014, a total of about 6700 h of operational experience had been published from more than 20 different test units [18]. Less than 20% of that experience came from solid fuels [19], the rest mostly from gaseous fuels. The total operational time published with liquid fuels is less than 400 h, which corresponds to less than 6% of all operational experience. The majority of this experience, more than 300 h, comes from the work included in this thesis. It should also be mentioned that when this research project started, there was very limited work on chemical-looping combustion with liquid fuels available, and no reports on operation with direct and continuous injection of liquid fuel to the fuel reactor.

### 1.1.1 Chemical-Looping with Oxygen Uncoupling

Chemical-looping with oxygen uncoupling (CLOU) is a variant of chemical-looping combustion. After the oxidation of oxygen carrier in the air reactor, according to Reaction (R1), the oxidized oxygen carrier is transported into the fuel reactor, where it releases oxygen in gaseous form, see Reaction (R3). Reactions between fuel and gas-phase oxygen, as in Reaction (R4), could be much faster than the corresponding CLC reaction, where fuel reacts with oxygen that is bound to the solid oxygen carrier.



One mechanism for oxygen release is a phase change of the oxygen carrier between air reactor and fuel reactor, e.g.  $2 \text{CuO} \rightleftharpoons \text{Cu}_2\text{O} + 1/2 \text{O}_2(\text{g})$ . The phase change, in turn, is

triggered by a change in oxygen partial pressure and/or temperature. Whether or not a CLC process is also a CLOU process is determined by the properties of the oxygen carrier, i.e. its ability to undergo phase changes under prevailing conditions. In addition to oxygen release through actual phase change, certain materials, such as calcium-manganite perovskites, can release oxygen to the gas phase without undergoing a change of solid phase [20]. Instead, this material can release oxygen through oxygen conduction, which depends on the surrounding partial pressure of oxygen as well as the temperature.

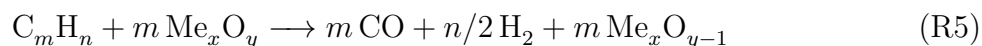
Although oxygen uncoupling could be advantageous for all types of fuel, it is for combustion of solid fuel where the most obvious advantages exist. This is because the intermediate char gasification reactions are partly or totally eliminated, and “replaced” by a combustion step [21]. For liquid fuel, the use of a CLOU material is expected to show a clear improvement in fuel conversion for a number of reasons.

1. In a well-mixed bed, there will be oxygen released at the top of the bed, which can oxidize gas that bypasses the bed in bubbles. Hence, it is very likely that much less oxygen-carrier material will be needed in order to fully oxidize the fuel.
2. Deposition of char, which is expected when solid fuels or heavy oil fractions are used, could become less problematic as carbon would be burned-off by gaseous oxygen.
3. If the oxygen release is rapid, the overall reaction will be governed by the normal combustion reaction, which is likely more rapid than the gas–solid reaction occurring in normal chemical-looping combustion.
4. In chemical-looping combustion and for a first order reaction, the gas yield as a function of bed mass can be expected to approach full conversion asymptotically. This means that a much higher relative bed mass will be needed in order to convert the last remnants of the fuel [22]. This is not the case with CLOU in a fluidized bed, where the oxygen release in the presence of fuel would be approximately proportional to the bed mass and in principle independent of the concentration of gaseous reactants. Thus, the bed mass needed to reach full fuel conversion is potentially much lower with CLOU as compared to CLC.

### 1.1.2 Chemical-Looping Reforming

Chemical-looping reforming (CLR) is a process derived from chemical-looping combustion. Just like in CLC, oxygen is transported between two reactors by solid oxygen-carrier particles. The difference compared to CLC is that insufficient amounts of air are added to the air reactor to convert the fuel to  $\text{CO}_2$  and  $\text{H}_2\text{O}$ . Instead, the product is a synthesis gas that consists mainly of  $\text{CO}$  and  $\text{H}_2$  [23].

The reaction in the air reactor is the same as for chemical-looping combustion, see Reaction (R1). Typically, all oxygen is taken up by the oxygen carrier so that the off-gas from the air reactor will consist almost completely of  $\text{N}_2$ . While it is unavoidable that some fuel is fully oxidized according to Reaction (R2), the major part is partially oxidized according to Reaction (R5).



H<sub>2</sub>O or CO<sub>2</sub> could be added to the fuel reactor in order to adjust the H<sub>2</sub>/CO ratio in the synthesis gas produced in accordance with Reactions (R6) and (R7), respectively [24].



The syngas produced can be further processed in order to generate hydrogen. In this case, the chemical-looping reforming process is succeeded by a water–gas shift reaction and subsequent CO<sub>2</sub> capture, e.g. through pressure swing adsorption.

### 1.1.3 Chemical-Looping Combustion with Liquid Fuel

As was mentioned previously in Section 1.1, most work around CLC has focused on gaseous and solid fuels, with very little experiments performed using liquid fuels. Gaseous fuels are easier to handle and process than liquid fuels and can be used to fluidize the oxygen carrier in the fuel reactor, which reduces the complexity of the process. Thus, gaseous fuels were used when the technology was new and little experience was available. However, it is not clear whether chemical-looping combustion with gaseous fuels can gain acceptance on a large scale. In electric power generation, combined-cycle power plants fired with natural gas can achieve efficiencies clearly above 50%. With a chemical-looping process, such power-generation efficiencies could be achieved if air reactor and fuel reactor would be pressurized and combined with a gas turbine process, see, e.g., [25, 26]. A pressurized chemical-looping process implicates technical challenges and it is not clear whether such a process can be technical feasible on a large scale. Solid fuels are cheaper and more abundant than liquid fuels and are probably the economically most feasible choice for a commercial chemical-looping process.

Liquid fuels have a high energy density and are therefore mostly used for transportation. In electric power generation, the global share of oil fell from 7.8% to 4.6% between the years 2000 and 2010, and was at 5.0% in 2012 [27, 28]. In an oil refining process, a large variety of end products can be generated, which differ greatly in quality and price. Low-grade heavy-oil products, such as vacuum residues, are upgraded if economically feasible. Such low-grade products, however, could pose an interesting and feasible option for combustion processes, especially if the process is located close to, or integrated in, a refinery process, where there is a constant need for heat and steam. Difficulties in the use of heavy-oil products are related to handling, because of their high viscosity, and to high amounts of sulphur and other impurities, such as heavy metals.

Research that focuses on the use of liquid fuels in chemical-looping combustion is very limited, which reflects on the number of publications available. Forret et al. [29] and Hoteit et al. [30] tested different fuels, namely *n*-dodecane, fuel oil and heavy fuel oil, in a batch fluidized-bed reactor with direct injection of liquid fuel. Cao et al. [31] gasified asphalt and bitumen in an upstream process, before burning the product gas in a batch fluidized-bed reactor. Bao et al. [32] saturated a flow of nitrogen with *n*-heptane, which was then fed to a batch fluidized-bed reactor. Chiu et al. [33] mixed isopropanol with water and used nitrogen as a carrier gas to convey the evaporated fuel into a moving-bed reactor. As part of this thesis, experiments were performed with different oxygen-carrier materials and sulphurous and sulphur-free kerosene as fuel. The fuel was evaporated, mixed with steam and fed into a bench-scale chemical-looping reactor with continuous circulation of oxygen-carrier particles [15, 34, 35]. Subsequently, this process was scaled up to pilot scale with direct injection of fuel oil 1 into the fluidized bed of the fuel reactor [36]. After some adaptations of the injection system, different blends of a vacuum residue and fuel oil 1 could be fed into the fuel reactor. A recent publications by Serrano et al. reports the construction of a chemical-looping reactor system for continuous operation with liquid fuels [37]. The system has a nominal capacity of 1 kW<sub>th</sub> and in the first results published, different oxygen-carrier materials were tested with ethanol as fuel.

A summary of all publications available that focus on chemical-looping with liquid fuels, i.e. combustion and reforming, is given in Table 1.1.

**Table 1.1:** Publications with focus on chemical-looping combustion/reforming with liquid fuels

Authors, reference and year of publication	Reactor type and size	Combustion or reforming	Fuels investigated	Comments
Forret et al., 2009 [29] and Hoteit et al., 2011 [30]	Batch fluidized-bed reactor, ID 20 mm	Combustion	<i>n</i> -dodecane ( $C_{12}H_{26}$ ), fuel oil and heavy fuel oil	
Pimenidou et al., 2010 [38, 39]	Batch packed-bed reactor, ID 20.5 mm, H 269 mm	Reforming	Waste cooking oil	Focus on production of hydrogen
Lea-Langton et al., 2010 [40], 2012 [41] and Gianakeas et al., 2012 [42]	Batch packed-bed reactor	Reforming	Waste lubricating oil, two biomass pyrolysis oils and scrap tyre pyrolysis oil	Focus on production of hydrogen
Cao et al., 2011 [31]	Batch fluidized-bed reactor, ID 20 mm	First reforming then combustion	Bitumen and asphalt	Gasification in separate reactor then combustion of synthesis gas
Mendiara et al., 2011 [43]	Batch fixed-bed reactor, ID 17 mm, H 610 mm	Reforming	Nitrogen saturated with toluene ( $C_7H_8$ )	Focus on tar reforming
Moldenhauer et al., 2012 (Paper II) [15]	Circulating fluidized-bed reactor, FR 25 × 25 mm, H 212 mm	Reforming	Sulphur-free kerosene	
Moldenhauer et al., 2012 (Papers II–III) [15, 34], 2014 (Paper IV) [35]	Circulating fluidized-bed reactor, FR 25 × 25 mm, H 212 and 300 mm	Combustion	Sulphur-free and sulphurous kerosene	Two reactors w/ different heights were used
Bao et al., 2013 [32]	Batch fluidized-bed reactor, ID 20 mm and TGA	Combustion	Nitrogen saturated w/ heptane ( $C_7H_{16}$ )	

continued on next page ...

Table 1.1 – continued from previous page

Authors, reference and year of publication	Reactor type and size	Combustion or reforming	Fuels investigated	Comments
Iliuta and Iliuta, 2013 [44]	Numerical study	Combustion and reforming	Glycerol ( $C_3H_8O_3$ )	
Wang, 2014 [45]	Batch fixed-bed reactor, ID 10 mm, H 300 mm	Reforming	Ethanol ( $C_2H_6O$ )	Also: thermodynamic study
Zhang et al., 2014 [46]	–	Reforming	Bio oil	Only particle characterization; focus on production of hydrogen
Chiu et al., 2014 [33]	Moving-bed reactor, ID 76.2 mm, H 900 mm	Combustion	2-Propanol ( $C_3H_8O$ )	
Moldenhauer et al., 2014 (Paper V) [36]	Circulating fluidized-bed reactor, FR ID 150 mm, H 2 m	Combustion	Diesel-type fuel oil 1	
Serrano et al., 2014 [37] and García-Díez et al., 2014 [47]	Circulating fluidized-bed reactor, FR ID 26→85 mm, bed height 150 mm	Combustion and reforming	Ethanol ( $C_2H_6O$ )	

---

## 1.2 Aim and Scope

The main focus of this thesis is the implementation and scale-up of chemical-looping combustion with liquid fuels. The final aim was to inject a type of heavy fuel oil, i.e. vacuum residue, directly into the fuel reactor of a pilot-scale chemical-looping reactor. Vacuum residue can be a by-product in an oil refinery process and is a potentially cheap fuel. However, it has a very high viscosity at room temperature and contains a considerable amount of sulphur and heavy metals. Prior to this study, liquid fuels had never been used directly and continuously in chemical-looping combustion. Thus, the project was divided into several sub-parts.

1. Design and operation of a bench-scale reactor for liquid fuels with continuous circulation of oxygen carrier.
  - a) Testing of a number of oxygen-carrier materials with a model liquid fuel, i.e. kerosene.
2. Design and operation of a pilot-scale reactor with direct and continuous injection of liquid fuel.
  - a) Long-term operation with a fuel oil using a promising oxygen carrier from 1a) above.
  - b) Operation with a vacuum residue that originates from Saudi Arabia.

## 1.3 Content of the Thesis

This thesis is based on experimental work, which was performed at Chalmers University of Technology in different circulating fluidized-bed reactors. The focus lies on the use of liquid fuel in chemical-looping combustion. In two different chemical-looping reactors, fuel powers from  $140 W_{th}$  up to  $6 kW_{th}$  were tested. The liquid fuels used, are a sulphur-free and a sulphurous kerosene, a diesel-type fuel oil 1 and different blends of vacuum residue with fuel oil 1. The experimental progress of the work in this thesis is depicted in Figure 1.2 through the experimental parameters, fuel power and distillation temperature of fuel.

Chapter 1 gives an introduction to the topic and describes the aim of the research. Chapter 2 describes the experimental setup, which includes the chemical-looping reactor, the measurement system, fuels and oxygen carriers used, and the experiments conducted. The results are summarized and discussed in Chapter 3 and the final part of this thesis, Chapter 4, provides the main conclusions of the work.

In Paper I, a mineral, ilmenite, and an industrial by-product, iron-oxide scale, are investigated with syngas as fuel. Both oxygen carriers are cheap and potentially abundant. Syngas, which consisted of 50 vol%  $H_2$  and 50 vol%  $CO$ , is an intermediate combustion product of liquid and solid fuels. Especially the ilmenite oxygen carrier worked well over long operating periods and showed promising results, which made further investigation with liquid fuel reasonable.

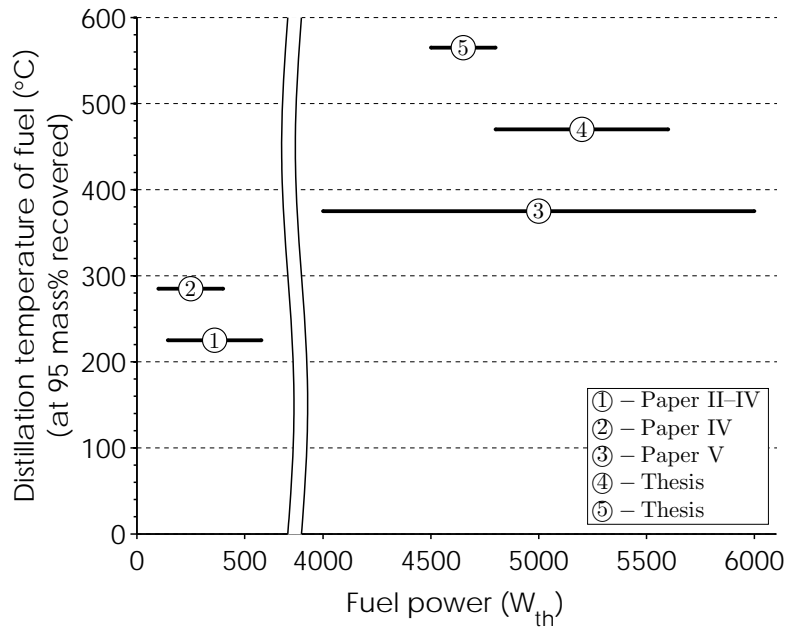


**Figure 1.2:** Experimental progress illustrated through experimental parameters fuel power and distillation temperature of fuel (at 95 mass% recovered).<sup>1</sup> Each number corresponds to one liquid fuel that was used.

Paper II is a proof-of-concept paper on the use of liquid fuel in a chemical-looping reactor with continuous circulation of oxygen carrier. A nickel-based oxygen carrier was used due to its good conversion properties for gaseous fuels. Both chemical-looping combustion (CLC) and chemical-looping reforming (CLR) experiments were performed with a sulphur-free kerosene as fuel. The oxygen carrier was analyzed before and after the experiments using XRD, SEM, BET surface area measurements and particle size distribution. For CLC, nearly complete fuel conversion was achieved with virtually no hydrocarbons left in the flue gases. For CLR, a synthesis gas was produced with a hydrocarbon content as low as 0.01 vol%.

Paper III continues the work of Paper II by investigating the conversion properties of sulphur-free kerosene with two more oxygen carriers, a manganese-based material and a copper-based material. At typical CLC conditions, copper-based oxygen carriers release gas-phase oxygen in the fuel reactor, which allows potentially higher fuel conversion compared to a regular oxygen-carrier material. Both oxygen carriers showed good results, though clearly higher fuel conversion to  $CO_2$  and  $H_2O$  was achieved with the copper-based material.

In Paper IV, an ilmenite oxygen carrier was tested with a sulphur-free kerosene and a kerosene that contained about 0.57 mass% of sulphur. This paper is an advancement towards the goal of using heavy liquid fuels with high sulphur content. Attempts were made to measure the sulphur species  $H_2S$  and  $SO_2$  in the flue gases and it was found that the

<sup>1</sup>The distillation temperatures of the blends of vacuum residue and fuel oil 1 are calculated by linear interpolation with respect to the blending ratio. Vacuum residue cannot be distilled like lighter hydrocarbons and, therefore, the distillation temperature was approximated.

---

conversion of sulphur to  $\text{SO}_2$  follows that of carbon to  $\text{CO}_2$ , which was also supported by thermodynamic equilibrium calculations. During the experiments, a significant and lasting improvement in the oxygen carrier's reactivity was observed when sulphurous kerosene was used. Surface measurements on the ilmenite particles were performed after the experiments but there was no evidence for the presence of sulphur. Another thermodynamic equilibrium calculation was performed, which showed that sulphur is unlikely to form on ilmenite oxygen carrier under typical chemical-looping conditions.

Paper V presents the commissioning of an injection system for liquid fuels and long-term tests in a pilot-scale chemical-looping reactor. The unit, which has previously been used with gaseous fuel, includes high velocity distributor nozzles and a riser section, and hence, the particles are exposed to relatively high velocities, similar to those encountered in industrial circulating fluidized-bed boilers. In this setup the fuel, a diesel-type fuel oil 1, was fed directly and as a liquid into the fluidized bed of the fuel reactor. For the commissioning process, a calcium manganite-based oxygen carrier with a perovskite structure and oxygen release properties was used. Subsequently, long-term experiments with an ilmenite oxygen carrier were performed, with about 70 h of fuel injection and more than 200 h of fluidization in hot state. The ilmenite oxygen carrier was very stable and only minor amounts of fines were produced. Fuel oxidation of up to 87% was achieved.

In addition to the results published in Paper I-V, this thesis presents results with ilmenite oxygen carrier and two different blends of vacuum residue and fuel oil 1 in the pilot-scale reactor.



---

## 2 Experimental Details

---

### 2.1 Chemical-Looping Reactors

Two different types of chemical-looping reactors were used. Different versions of a bench-scale reactor with a nominal fuel power of  $300 \text{ W}_{\text{th}}$  were used for the experiments described in Papers I–IV. A pilot-scale reactor with a nominal fuel power of  $10 \text{ kW}_{\text{th}}$  was used for the work in Paper V and for further experiments presented in this thesis.

#### 2.1.1 Bench-Scale Reactor

The working principles of the two bench-scale chemical-looping reactors used, are shown in Figure 2.1. Both reactors have a similar design and the same nominal fuel power of  $300 \text{ W}_{\text{th}}$ . Version 3 of the reactor, see Figure 2.1b, was designed and constructed as part of this thesis, while version 2 has been used previously for combustion of gaseous fuels [24, 48, 49]. Both units have the advantage of being highly compact, and hence, it is possible to test rather small quantities of oxygen-carrier particles, typically 100–400 g, in continuous circulation.

Fuel and air enter the system through separate windboxes, located in the bottom of each reactor. Porous quartz plates act as gas distributors. In the air reactor, the gas velocity is sufficiently high to create a circulating fluidized-bed and oxygen-carrier particles are thrown upward. The particle–gas mixture is then separated: oxygen-depleted air is returned to the atmosphere, whereas a fraction of the particles falls into the standpipe of the downcomer, which is the inlet of a J-type loop seal. From the loop seal, particles overflow into the fuel reactor via the return orifice. The fuel reactor is a bubbling-bed counterflow reactor, i.e. particles move downward, while gas moves upward. From the bottom of the fuel reactor, particles flow into the underflow standpipe of the slot, which is essentially a U-type loop seal, and return to the air reactor, where the whole cycle starts over again. The exit pipe of the fuel reactor is connected to a water seal, which has a column height of 1–2 cm. As a result, the pressure in the fuel reactor is 0.1–0.2 kPa higher than in the air reactor, which reduces gas leakage from air reactor to fuel reactor.

Oxygen-carrier particles in the air reactor are fluidized with air, and reduced particles,  $\text{Me}_x\text{O}_{y-1}$ , are oxidized to  $\text{Me}_x\text{O}_y$  according to Reaction (R1). In the fuel reactor, the particles are fluidized by gas-phase fuel or, in case of kerosene, a gaseous steam–fuel mixture.

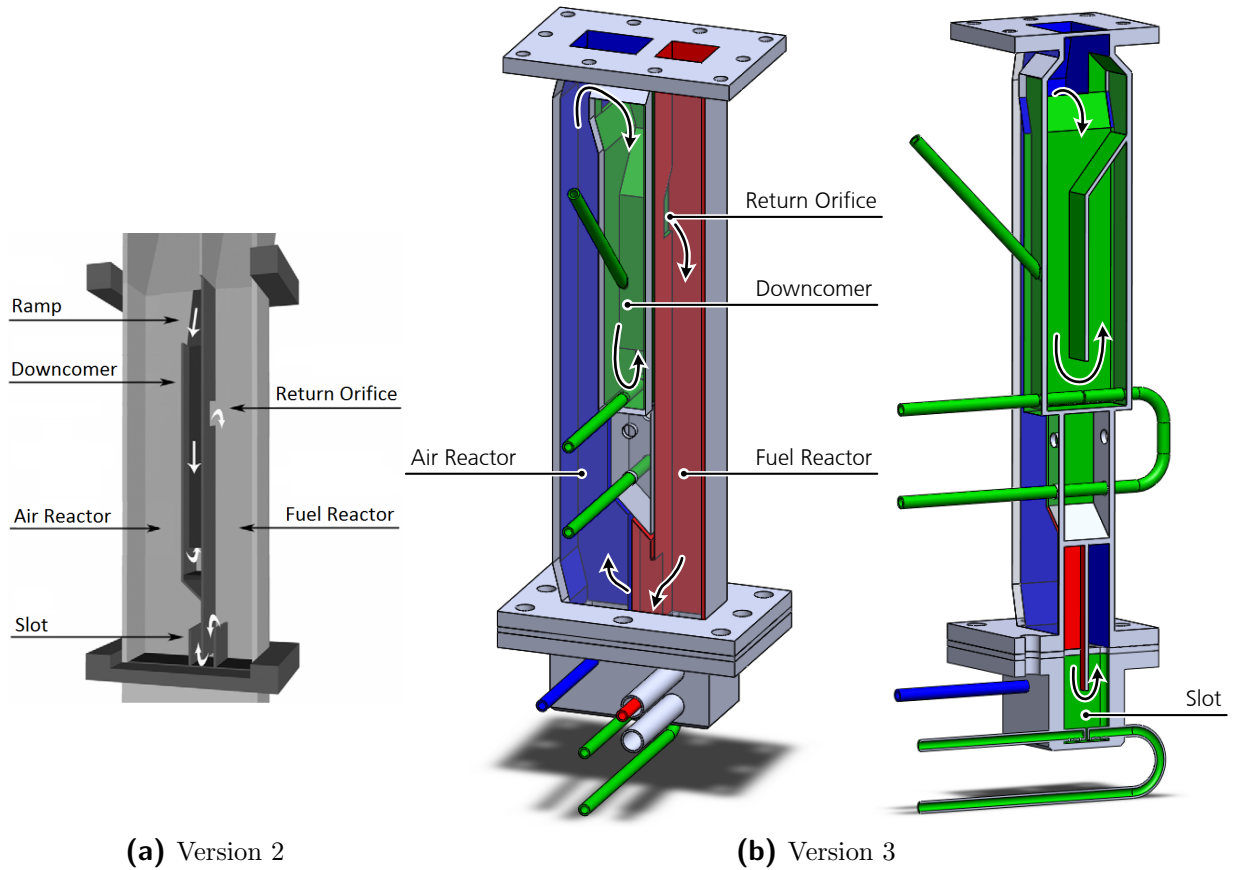


**Figure 2.1:** True-to-scale representation of the two versions of the bench-scale chemical-looping reactor

Particle reduction occurs either directly by fuel, according to Reaction (R2), or, if a CLOU oxygen carrier is used, indirectly through released oxygen, as in Reaction (R3). In this reactor, both loop seals are fluidized with argon.

Version 3 of the reactor is a further development of version 2 with the following improvements:

- Increased height of air reactor and fuel reactor in order to gain more flexibility regarding solids inventory.
- Improved slot design in order to reduce gas leakage and enhance circulation.
- Improved downcomer design in order to enhance circulation.

Version 2 of the reactor, see Figure 2.1a, was used for the experiments with ilmenite oxygen carrier and syngas as fuel, see Paper I [49], and with nickel-based oxygen carrier and liquid fuel, see Paper II [15]. Version 3, see Figure 2.1b, was used for all other materials with kerosene, i.e. Papers III–IV [34, 35]. The main dimensions of both reactor versions are summarized in Table 2.1.

---

**Table 2.1:** Main dimensions of versions 2 and 3 of the bench-scale reactor

Reactor part	Dimension (mm)	
	Version 2	Version 3
Reactor height	212	300
Fuel reactor area	$25 \times 25$	$25 \times 25$
Air reactor bottom area	$45 \times 25$	$42 \times 25$
Air reactor riser area	$25 \times 25$	$25 \times 25$
Downcomer height	75	83
Downcomer area	$16 \times 11.5$	$21 \times 21$
Slot height	18	48
Slot area	$7.5 \times 25$	$10 \times 11.5$

Due to the small thermal output, the heat of reaction is not enough to generate a sufficiently high temperature. Therefore, the reactor is encased in an electric furnace, which allows operation up to about 1050°C.

## 2.1.2 Pilot-Scale Reactor

Figure 2.2 shows a schematic and the dimensions of the pilot-scale reactor system with all major sections, including gas and fuel inlets, and gas exits. The unit is based on interconnected fluidized beds and is similar to the design originally presented by Lyngfelt et al. [50]. It was designed for a fuel input of 10 kW<sub>th</sub>. In the riser section, there is a fast-fluidized regime, whereas in the loop seals and the fuel reactor, there is a bubbling regime. In the air reactor, the fluidization regime is on the transition between bubbling and fast-fluidized. The unit is equipped with heating cables, which are wrapped around the riser section, the cyclone, the upper loop seal and the fuel reactor, and covered with insulation material. Heating cables are needed in order to compensate for radiation losses at high temperatures, which are inherent in small-scale units like the one used here, i.e. such with a high ratio of surface area to volume. Additionally, the air that is fed to the air reactor is preheated to 1000°C.

The amount of oxygen carrier used in the 10 kW unit depends on the bulk density of the oxygen-carrier particles. In the configuration used for injection of liquid fuel, the bed mass is roughly in the range of 15–25 kg, out of which 5–10 kg are in the fuel reactor. The relatively large amounts of material needed, make this unit unsuitable for screening of oxygen-carrier particles. On the other hand, the unit utilizes much higher gas velocities as compared to the bench-scale reactor. The superficial gas velocities in the riser and at the inlet of the cyclone are about 2–3 m/s and 5–7 m/s, respectively. At the outlet of the gas distributors in the the bottom of the air reactor, the gas velocity is around 25–35 m/s. These velocities are comparable to those in large-scale circulating fluidized-bed applications. Thus, this unit can give relevant information on particle behavior and performance at realistic conditions.

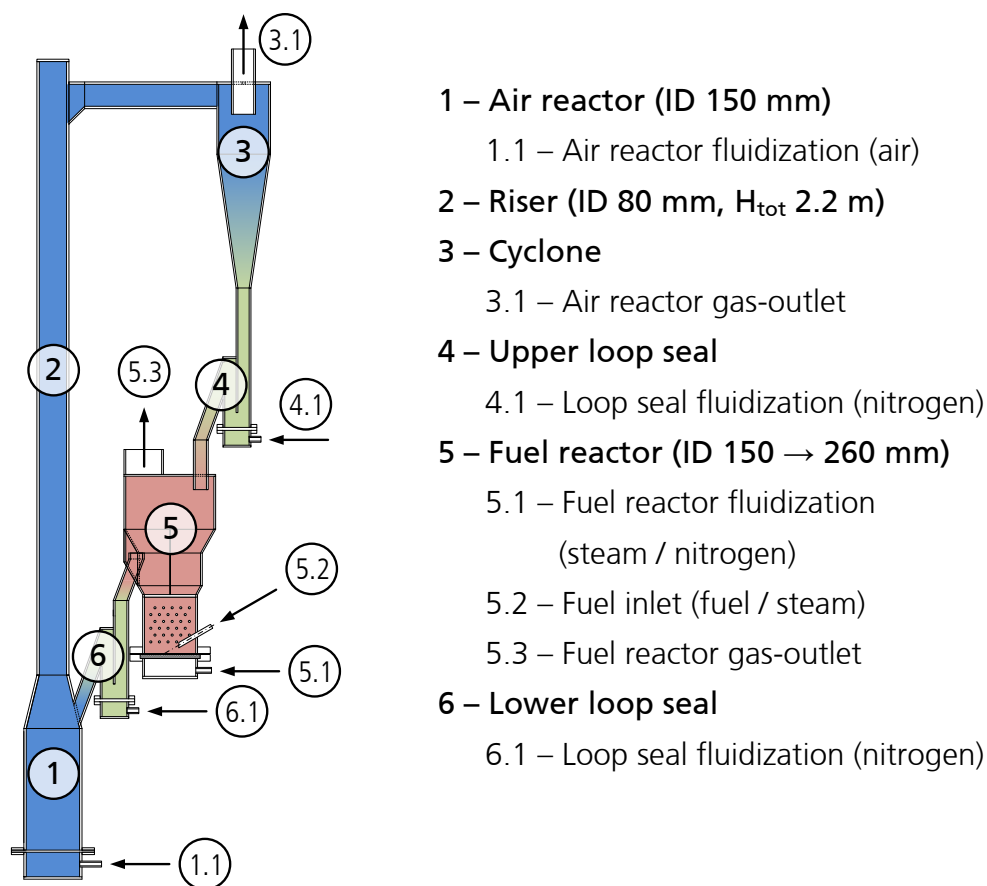


Figure 2.2: Schematic and main dimensions of the pilot-scale reactor

## 2.2 Liquid Fuels

In the work for Papers II–IV, two kinds of kerosene were used [15, 34, 35]. Paper V describes experiments with a fuel oil 1 [36], and in this thesis, experiments with a blend of a vacuum residue and fuel oil 1 are presented.

### 2.2.1 Kerosene

Two similar types of kerosene were used, i.e. a sulphur-free kerosene and a sulphurous kerosene, which were provided by courtesy of Preem AB in Gothenburg, Sweden. Both kerosenes were analyzed in a gas chromatograph (GC) with the simulated distillation method according to ASTM standard D 2887, which is a standard test method for boiling range distribution of petroleum fractions, see Figure 2.3. It was found that 95 mass% of the sulphur-free and the sulphurous kerosene is evaporated below 225°C and 285°C, respectively. Some of the peaks in the chromatogram coincide with those of linear alkanes. The most prominent peaks in the chromatogram of the sulphur-free kerosene coincide with *n*-C10 and *n*-C11. The sulphurous kerosene consists of much heavier components and here,

the most prominent peak coincides with that of *n*-C16. It is likely that the kerosenes not only contain linear alkanes but also branched iso-alkanes and possibly cyclic alkanes. An elemental analysis was performed, which suggests the presence of aromatic hydrocarbons. Alkenes and alkynes are rather unlikely in refinery products based on mineral oil. Table 2.2 shows results of the different analyses performed on the two types of kerosene and the other fuels used.

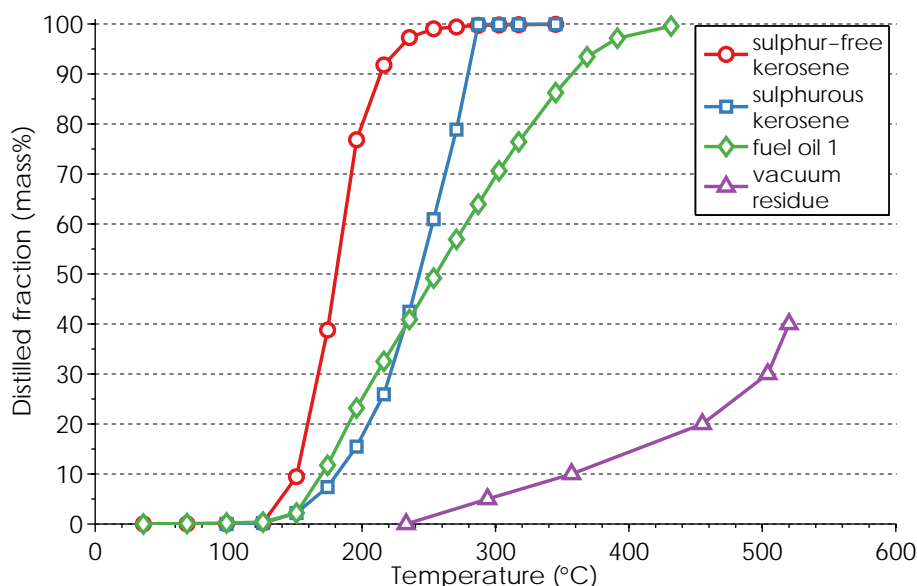


**Figure 2.3:** Boiling range distribution of the different liquid fuels used: sulphur-free kerosene, sulphurous kerosene, fuel oil 1 and vacuum residue.<sup>2</sup>

<sup>2</sup>The boiling range distributions of sulphur-free kerosene, sulphurous kerosene and fuel oil 1 were determined according ASTM standard D 2887. The boiling range distribution of vacuum residue was determined in vacuum according to ASTM standard D 1160, which includes the calculation of atmospheric equivalent temperatures that are used here.

**Table 2.2:** Results of the analysis on the different liquid fuels used: sulphur-free kerosene, sulphurous kerosene, fuel oil 1 and vacuum residue.

Analysis parameter	Unit	Fuel type			Analysis method
		Sulphur-free kerosene	Sulphurous kerosene	Fuel oil 1	
Carbon content	mass%	86.2 ± 0.5	85.9 ± 0.5	86.6 ± 0.5	ASTM D 5291
Hydrogen content	mass%	13.5 ± 0.4	13.5 ± 0.4	13.7 ± 0.4	ASTM D 5291
Nitrogen content	mass%	<0.1 ± 0.03	<0.1 ± 0.03	<0.1 ± 0.03	ASTM D 5291
Sulphur content	mg/kg	<1	5700 ± 400	<500 ± 40	ASTM D 1552
Ash content	mg/kg	not tested	not tested	<100	ISO 6245 (FO1), ASTM D 482 (VR)
Vanadium content	mg/kg	–	–	not tested	ASTM D 5185
Nickel content	mg/kg	–	–	not tested	ASTM D 5185
Sodium content	mg/kg	–	–	not tested	ASTM D 5185
Lower heating value	MJ/kg	43.34 ± 0.21	42.66 ± 0.20	43.00 ± 0.21	ASTM D 240
Higher heating value	MJ/kg	46.20 ± 0.22	45.52 ± 0.22	45.91 ± 0.22	ASTM D 240
Density	kg/dm <sup>3</sup>	0.792 <sup>†</sup>	0.860 <sup>†</sup>	0.832 ± 0.001 <sup>‡</sup>	see footnotes
Hydrogen-to-carbon ratio	mol/mol	1.87 ± 0.07	1.87 ± 0.07	1.89 ± 0.07	calculated
Distillation temperature at 95 mass% recovered	°C	225	285	375	ASTM D 2887
				n/a <sup>§</sup>	

FO1 = fuel oil 1. VR = vacuum residue.

<sup>†</sup>measured at 20°C at atmospheric pressure<sup>‡</sup>measured at 15°C in vacuum according to ASTM D 4052<sup>§</sup>Vacuum residue cannot be fully distilled like lighter hydrocarbons because of initiation of thermal cracking, which leads to fouling.

---

## 2.2.2 Fuel Oil

The fuel oil 1 used is a diesel-type fuel oil with low sulphur content. This type of fuel is usually used as domestic heating/fuel oil. The fuel's commercial name is Eo1 E10 and was purchased from a local provider, Preem AB in Gothenburg, Sweden. It meets the requirements for fuel oil defined in the Swedish standard SS 155410. An elemental analysis was performed, and density and heating values were measured, see Table 2.2. Additionally, a boiling range distribution was determined according to ASTM standard D 2887, see Figure 2.3. 95 mass% of the fuel has an evaporation temperature below 375°C. The fuel contains about 15 vol% aromatic compounds.

## 2.2.3 Vacuum Residue

Vacuum residue is the bottom product of a vacuum distillation in an oil refinery process. Prior to vacuum distillation, crude oil is fractionated in a crude distillation unit, which operates at atmospheric pressures. The residue of the crude distillation unit is used as feedstock for a vacuum distillation unit, where the vacuum residue is obtained. Vacuum residue is an intermediate and low-value product that can be either converted to asphalt in an asphalt blower or upgraded in a delayed coking process to more valuable products, like naphtha or gas oils. The by-product from this upgrading process is petroleum coke. A comprehensible and illustrated summary of the different processes in an oil refinery can be found in [51]. A comprehensive report on heavy fuel oils, which have many similarities with vacuum residue, can be found in [52].

A vacuum residue, which was provided by courtesy of Saudi Aramco, Kingdom of Saudi Arabia, was blended with a fuel oil 1, cf. Section 2.2.2, and used as fuel. Vacuum residue generally has a high viscosity, which makes handling difficult. Additionally, it contains contaminants, like sulphur and different heavy metals, which can cause corrosion or fouling problems. The viscosities of the vacuum residue, the fuel oil 1 and different blends of both are shown in Figure 2.4. A boiling range distribution of the vacuum residue, performed at reduced pressure, is shown Figure 2.3, and further fuel properties can be found in Table 2.2.

As can be seen in Figure 2.4, blending the vacuum residue with the fuel oil 1 causes a dramatic reduction in viscosity. Hence, little or no heating is necessary in order to handle and pump the fuel. Using cold fuel instead of preheated fuel can be an important contribution towards a reduction in fuel temperature in the fuel injector. Above a certain temperature, ca. 350°C, thermal decomposition followed by polymerization can occur in the fuel [53], which can lead to blocking of the injector.

Two different blends of vacuum residue and fuel oil were prepared and used as fuel: a 40:60 blend (40 wt% vacuum residue in fuel oil) and a 80:20 blend (80 wt% vacuum residue in

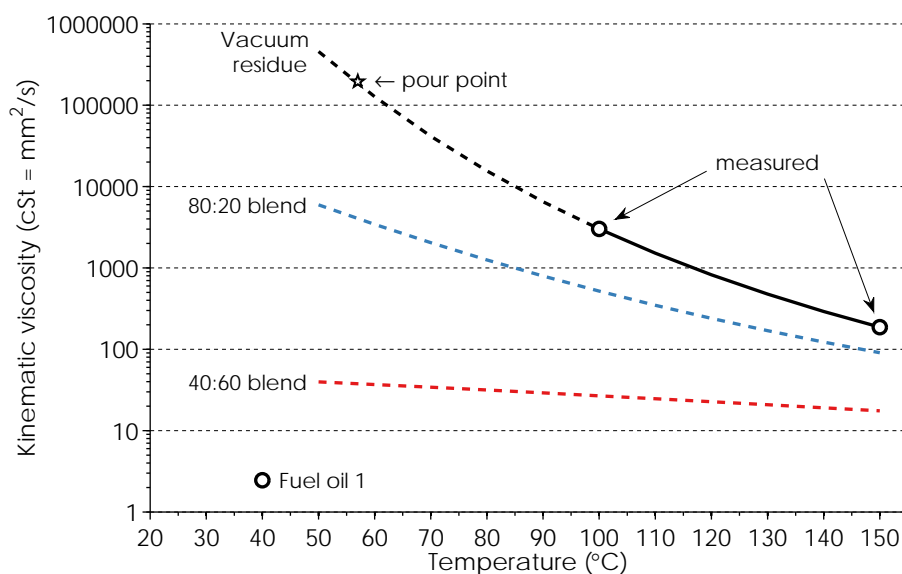


**Figure 2.4:** Kinematic viscosity at different temperatures of vacuum residue, fuel oil 1 and different blends of both. For vacuum residue, the pour point is shown.<sup>3</sup>

fuel oil). The 40:60 blend did not require any preheating, whereas the 80:20 blend was preheated to 30°C in the fuel tank and kept at that temperature in the feeding system.

## 2.3 Injection Systems for Liquid Fuel

As part of this thesis, injection systems were designed for the different fuels and chemical-looping reactors used. The injection principle for the two kinds of kerosene, which were used in the bench-scale reactors, differs fundamentally from the injection principle used for fuel oil 1 and vacuum residue, as is shown in the following sections.

### 2.3.1 Fuel Vaporization Concept

The basic principle of the injection system for the bench-scale reactor is to evaporate the liquid fuel, using superheated steam as heat source, and to inject the resulting steam–fuel gas mixture in the bottom of the fuel reactor, see Figure 2.5. Hence, the steam–fuel mixture is both reactants and fluidizing medium. This is most convenient, because it causes the least changes to the reactor system, which is designed for gaseous fuels. Injection from the bottom is also beneficial with respect to achieving a high gas yield to carbon dioxide, as the gas conversion is a function of the contact time between oxygen carrier and reactant.

<sup>3</sup>The viscosity of the vacuum residue and the fuel oil 1 were measured according to standards ASTM D 445 and ISO 3104, respectively. The kinematic viscosities of the blends of vacuum residue and fuel oil 1 were calculated according to [54]. The pour point is defined as the lowest temperature at which, upon cooling, movement of a liquid is observed and was determined according to ASTM standard D 97.

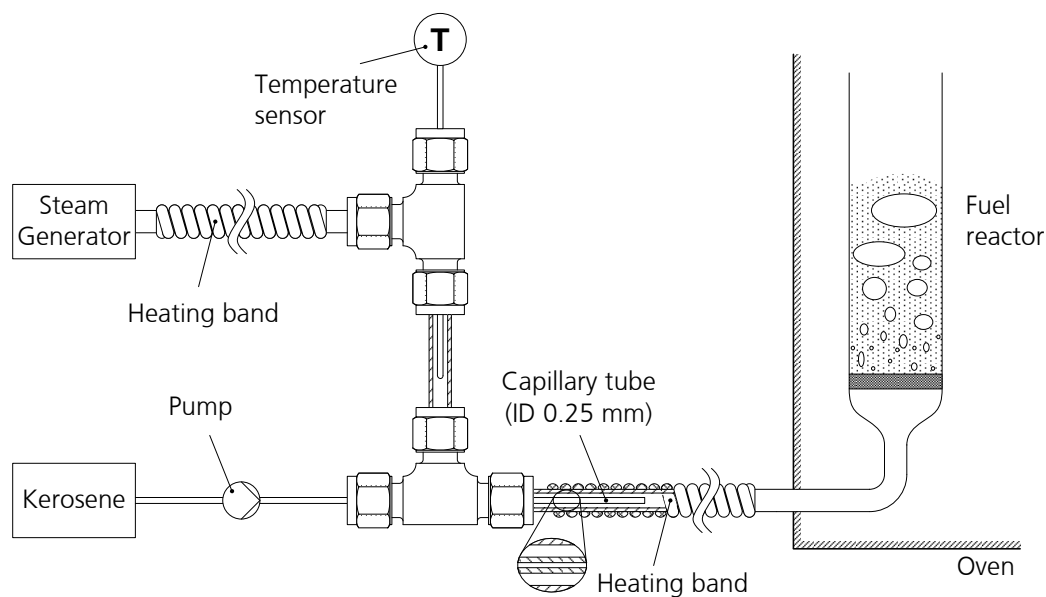


**Figure 2.5:** Schematic illustration of the injection system for kerosene

When the fuel molecules are converted, the gas volume is increased. Hence, the volume flow of the gaseous steam–fuel mixture is a function of the extent of hydrocarbons converted. The steam fulfills the secondary function of ensuring that enough gas is available to fluidize the particles in the fuel reactor. Poorly fluidized particles increase the risk of agglomeration, which may destroy the oxygen-carrier batch, depending upon the type of material used. Figure 2.5 shows how evaporation, mixing and injection are realized. Steam is generated continuously by a steam generator. A heating band is used to superheat the steam to the desired temperature, which is measured by a thermocouple temperature sensor. A continuous fuel flow is provided by a diaphragm metering pump. The fuel is fed through a capillary tube, which is concentrically arranged within the steam pipe. The heat necessary for evaporation of the fuel is thereby transported from steam to fuel.

With this injection system, a total of about 240 h of fuel operation were performed, out of which about 50 h were with sulphurous kerosene and the rest was with sulphur-free kerosene. Fuel fouling in combination with blocking of the injection system occurred only once and when sulphurous kerosene was used. Except for that, there were no problems with the injection system.

### 2.3.2 Direct Injection Concept

The lower section of the fuel reactor of the pilot-scale reactor, cf. Figure 2.2, was specifically designed for direct injection of liquid fuel, see Figure 2.6. The height of this section is about 165 mm and the bed diameter is 150 mm. The total bed height in the fuel reactor is 275 mm. Fuel is injected as a jet close to the center of the fluidized bed, and ca. 25 mm above the gas distributor plate. Internals are used to limit the growth of gas bubbles and to reduce

the risk of formation of gas channels, which would reduce the fuel–oxygen carrier contact and, therefore, decrease fuel conversion.

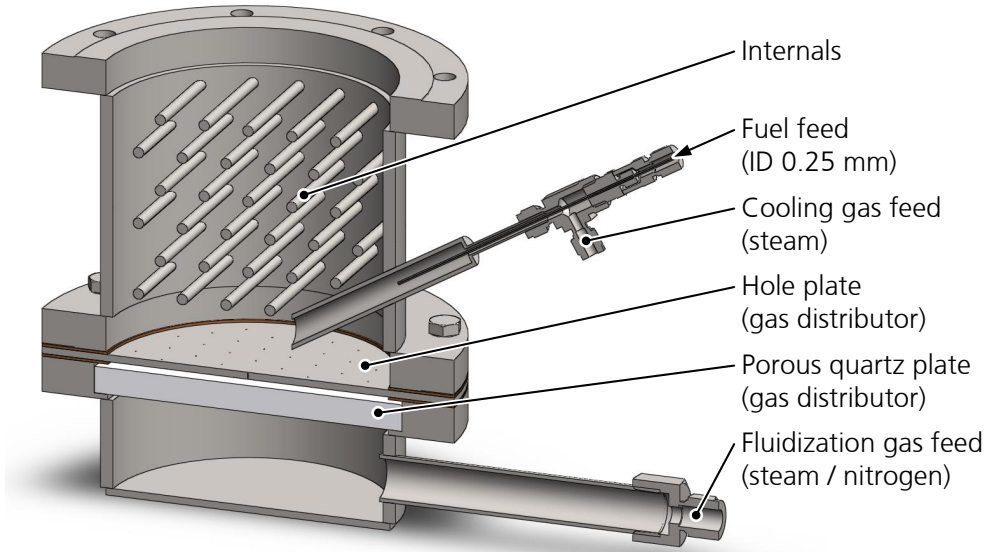


**Figure 2.6:** Lower fuel-reactor section for direct injection of fuel oil 1

In a first version of the injection system, see Figure 2.6, a long capillary is used to feed the fuel and to create a free fuel jet that extends to the fluidized bed. The inner diameter of the capillary is 0.25 mm. This diameter was chosen for a minimum fuel flow of  $6.7 \text{ ml}_{\text{liq}}/\text{min}$  ( $4.0 \text{ kW}_{\text{th}}$ ) in order to create a jet that stretches out over a distance of about 7 cm, without hitting the wall of the fuel injection system. The residence time of the fuel in the capillary is short and, hence, the fuel temperature at the tip of the capillary is kept low. Another benefit of using a capillary, i.e. an injection system with a distinct pressure gradient, is that fuel evaporation in the injection system is inhibited, cf. Figure 2.3, which could lead to unwanted pressure fluctuations. Steam is used to cool the fuel capillary and to keep oxygen-carrier particles from entering the fuel injection system. Upon shutdown, the fuel pump is switched off and the fuel injection system is purged with air in order to prevent fuel fouling during cool-down.

The pressure drop of the fuel over the fuel injection system was 4–10 bar for the different flows of fuel oil 1 used, i.e.  $6.6\text{--}10 \text{ ml}_{\text{liq}}/\text{min}$  ( $3.9\text{--}6.0 \text{ kW}_{\text{th}}$ ). The injection system worked flawlessly for the fuel oil used. During the single longest continuous test, fuel oil was injected for more than 12 h. The fuel injection system could be restarted, and there were no problems during a total fuel operation time of 66.6 h.

Using a long capillary to feed a fuel with a low viscosity, like the fuel oil 1 used, is a simple solution. However, using a capillary to feed heavier fuels would not have been technically feasible. The viscosity of the vacuum residue is about three orders of magnitude higher than that of the fuel oil 1, see Figure 2.4, and, hence, the pressure drop of the fuel over the injection system would have been impractical to handle. Therefore, the length of the capillary was reduced, while maintaining the inner diameter of 0.25 mm. After testing

different solutions, the fuel capillary was replaced with a tube with an outer diameter of 6 mm and an inner diameter of 1.7 mm, see Figure 2.7. On the tip of that tube, a replaceable customized fuel nozzle is attached. This modified injection system is a compromise between pressure drop and residence time of the fuel. It was tested with two different blends of vacuum residue and fuel oil, namely 40:60 and 80:20 by weight. Even with an increased flow of cooling steam, fouling of the fuel could not be inhibited completely. The longest continuous injection lasted just below one hour. The pressure drop of the fuel over the injection system was low, that is 4–8 bar, for the different flows of blended vacuum residue and fuel oil used, i.e. 7.0–8.6 ml<sub>liq</sub>/min (4.5–5.6 kW<sub>th</sub>).

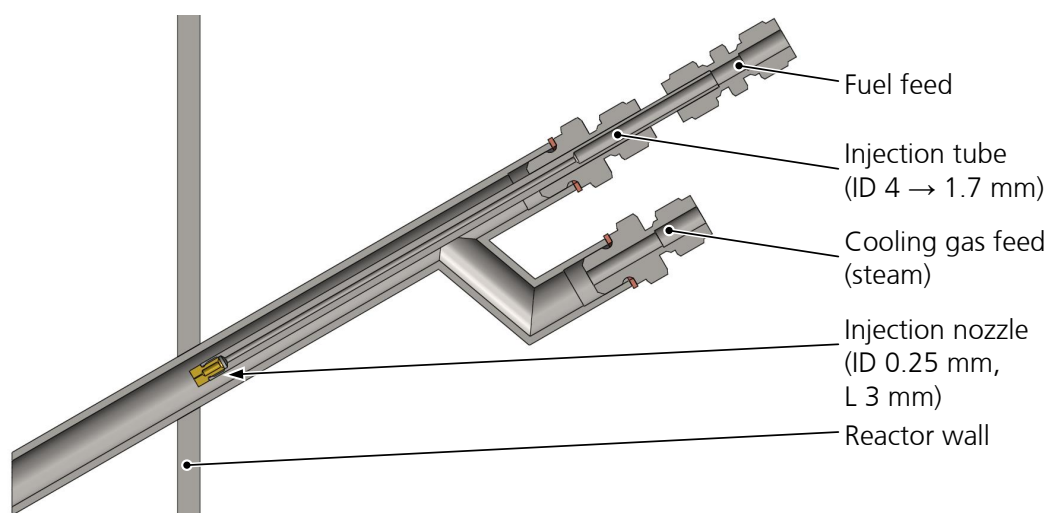


**Figure 2.7:** Fuel injection system adapted for vacuum residue

## 2.4 Measurements

The measurement systems used for the different reactor systems were very similar. During the experiments, measurements of pressure, temperature, gas flows and gas concentrations are logged continuously. For the experiments in the pilot-scale unit, the fuel flow is logged manually and is based on the measured weight of the fuel tank. For the experiments in the bench-scale unit, the fuel flow is metered directly by the fuel pump and logged manually.

Small streams of the flue gases from air reactor (AR) and fuel reactor (FR), ca. 1 L<sub>n</sub>/min on a dry basis, are diverted from the main gas streams, filtered, cooled to about 4°C and fed to gas analyzers. Gas concentrations of O<sub>2</sub> (paramagnetic sensor) and CO, CO<sub>2</sub> and CH<sub>4</sub> (infrared sensors) are measured continuously in the flue gases from both reactor vessels. A fraction of the dried gas stream of the fuel reactor is fed to a micro gas-chromatograph (GC) with two parallel columns (Molsieve MS5Å, 10 m × 0.32 mm and PoraPLOT Q, 10 m × 0.15 mm), which both are equipped with a thermal-conductivity detector. In the gas chromatograph, concentrations of H<sub>2</sub>, N<sub>2</sub>, O<sub>2</sub>, CO, CH<sub>4</sub>, CO<sub>2</sub>, C<sub>2</sub>H<sub>n</sub> and C<sub>3</sub>H<sub>n</sub><sup>4</sup> are detected

<sup>4</sup>C<sub>2</sub>H<sub>n</sub> and C<sub>3</sub>H<sub>n</sub> are substitute denominations for hydrocarbons with two and three carbon atoms, respectively. This includes the species C<sub>2</sub>H<sub>2</sub>, C<sub>2</sub>H<sub>4</sub>, and C<sub>2</sub>H<sub>6</sub> and C<sub>3</sub>H<sub>4</sub>, C<sub>3</sub>H<sub>6</sub>, and C<sub>3</sub>H<sub>8</sub>.

and quantified intermittently. Another small stream of the fuel reactor gases is kept above 155°C and analyzed separately and continuously in a flame ionization detector (FID), which measures the total carbon content in organic compounds, i.e.  $\sum (x \cdot C_x H_y O_z)$ . A schematic description of the system for gas analysis for the pilot-scale reactor can be found in Figure 2.8. The gas analysis system for the bench-scale unit is very similar to that of the pilot-scale reactor. However, there is no cyclone after the fuel reactor and, instead, particles are separated from the gas stream using a gravitational gas–solid separator.

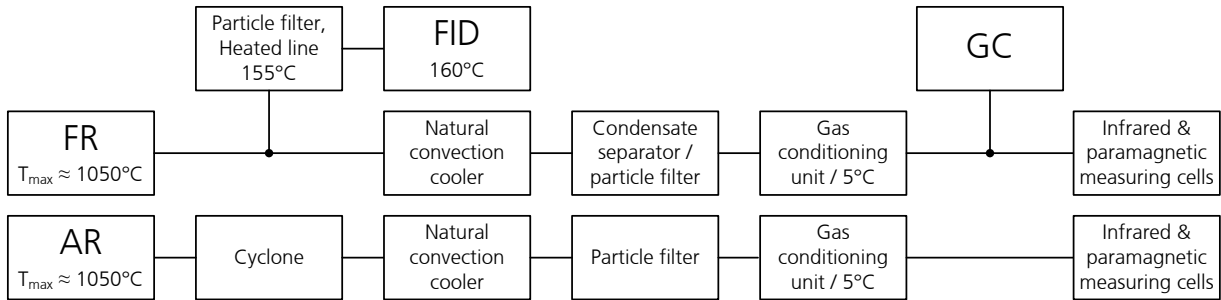


**Figure 2.8:** Schematic description of the gas-analysis system used for the pilot-scale unit

## 2.5 Oxygen Carriers

Different oxygen-carrier materials were selected for testing with liquid fuel. At the start of the project, there was very limited data available on liquid fuel reactions with oxygen-carrier materials. Hence, a wide range of different materials was selected on the basis of previous results with gaseous fuels. All materials are based on the transition metals nickel, manganese, iron and copper. All the materials listed in this section, except for the calcium manganite-based material,  $\text{CaMn}_{0.9}\text{Mg}_{0.1}\text{O}_{3-\delta}$ , were tested in the bench-scale reactor with sulphur-free kerosene. The materials that were found to be promising were then further tested with sulphurous kerosene. Ilmenite and the calcium manganite-based material were finally selected for testing in the pilot-scale reactor. This screening process is illustrated in Figure 2.9. During initial tests with syngas as fuel, ilmenite and iron-oxide scale were tested as oxygen carriers, see Paper I [49]. Iron-oxide scale, which is an iron-based waste product from the rolling of steel sheets, agglomerated on several occasions and was not considered for testing with liquid fuels.

### 2.5.1 Particle Preparation

The particle preparation method has a great impact on both the structural properties and the price of the particles produced. The two methods that were used to manufacture the oxygen-carrier particles used in this work are summarized in the following sections.

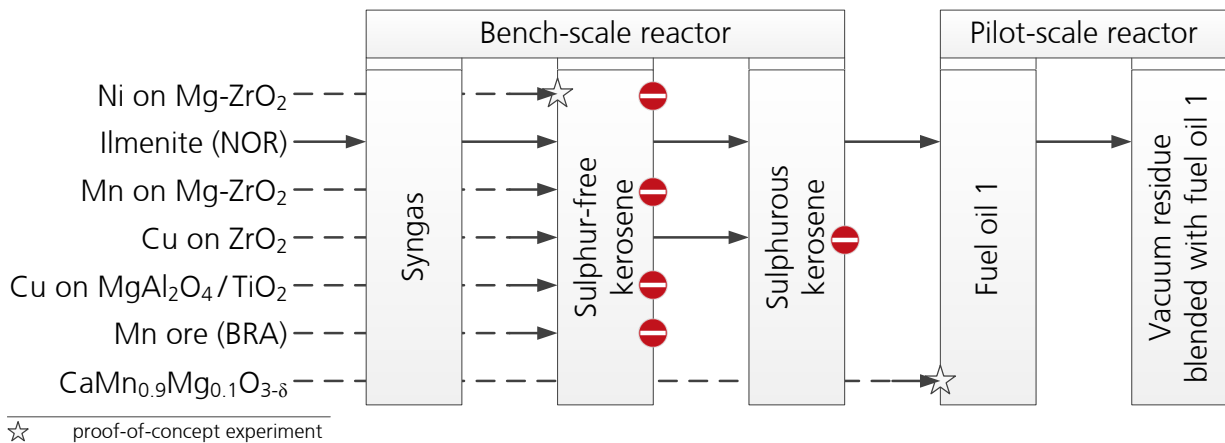


**Figure 2.9:** Experimental progress with focus on different oxygen-carrier materials tested

## Freeze-Granulation

A water-based slurry is prepared out of the milled raw materials. An organic binder is added to the slurry to bind the mixed raw materials together during later stages in the production process, i.e. freeze-drying and calcination. The slurry is dispersed in an atomizer nozzle, which produces spherical drops, and sprayed into liquid nitrogen, where the drops freeze instantaneously. The frozen water in the resulting particles is then removed by sublimation in a freeze-dryer. After drying, the particles are calcined to remove the binder and finally sieved to obtain particles in the desired size fraction. Typical calcination temperatures are 950–1400°C.

Freeze-granulation is a small-scale production method. Typically, batches of a few hundred grams are produced. The removal of water through freezing and sublimation produces regular spherical particles in a narrow size range.

## Spray-Drying

A water-based slurry is prepared out of the powdered raw materials and organic binder additives, and further homogenized by milling in a planetary ball mill. The water-based suspension is pumped through a spray nozzle, which produces spherical droplets, and into a stream of drying gas, where water is removed through evaporation. After spray-drying, the particles are sieved to the desired size fraction and calcined to remove the binder, typically at temperatures between 950°C and 1400°C.

Spray-drying is an established large scale production method. Fixed cost depression is valid, i.e. the larger the batch size produced, the lower the specific costs. Spray-drying produces spherical particles, which are, however, prone to defects like hollow or perforated (doughnut-shaped) particles.

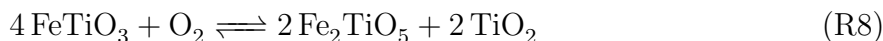
### 2.5.2 Synthetic Nickel-based Material

The nickel-based oxygen carrier used, N4MZ-1400, consists of 40 wt% NiO supported on 60 wt% Mg-stabilized ZrO<sub>2</sub>. The particles were produced through freeze-granulation with subsequent calcination at 1400°C by Swerea IVF in Mölndal, Sweden. Version 2 of the bench-scale reactor was initially filled with 250 g of N4MZ-1400 particles in the size range of 90–212 µm. Particles from the same batch have been used previously for CLC and CLR experiments with natural gas as fuel [55]. N4MZ-1400 was found to be a good oxygen carrier with high reactivity, structural stability and no fluidization problems. It is also an active catalyst for certain reactions, such as decomposition of hydrocarbons.

Nickel-based oxygen carriers also involve disadvantages. Besides health issues and the high price, nickel comes with thermodynamic limitations and never allows 100% conversion of any hydrocarbon-based fuel to CO<sub>2</sub> and H<sub>2</sub>O. Nickel is also known to suffer from poisoning/deactivation in presence of sulphur species at sufficient concentrations. The process is reversible but only if the oxygen carrier is treated in a sulphur-free atmosphere at a high temperature [56–58].

### 2.5.3 Mineral Ilmenite Material

Ilmenite is a mineral that consists mainly of iron–titanium oxides (FeTiO<sub>3</sub>) and some hematite (Fe<sub>2</sub>O<sub>3</sub>). To be used as an oxygen carrier, ilmenite is physically beneficiated and ground. In a chemical-looping process, ilmenite is usually assumed to be oxidized and reduced according to Reaction (R8).



It is known that ilmenite oxygen carrier undergoes structural changes as a consequence of continuous oxidation and reduction. The formation of a separate iron phase and its migration to the particle surface after several redox cycles has been reported in several publications [49, 59, 60]. Ilmenite has been studied in chemical-looping applications with solid fuels [61–64] and gaseous fuels [49, 59, 62, 65, 66]. Compared to synthesized oxygen carriers, ilmenite is relatively cheap, as no production step is needed to obtain the oxygen-carrier particles. The ilmenite used here was supplied by Titania A/S, Norway. It was 94.3 wt% pure and had a slight excess of iron, compared to stoichiometric ilmenite. About 380 g and 20–24 kg of ilmenite oxygen carrier, mainly in the size range of 90–250 µm, were used in version 3 of the bench-scale reactor and the pilot-scale reactor, respectively. The ilmenite oxygen carrier was tested with sulphur-free and sulphurous kerosene, fuel oil 1, and two blends of vacuum residue and fuel oil 1.

---

## 2.5.4 Synthetic Manganese-based Material

Manganese-based M4MZ-1200 consists of 40 wt%  $\text{Mn}_3\text{O}_4$  supported on 60 wt%  $\text{ZrO}_2$ , which was partially stabilized with MgO. Mixing active and inert material is a common way of increasing the reactivity and, in certain instances, the mechanical stability. Particles of this material were produced by VITO NV in Mol, Belgium, through spray-drying with subsequent calcination at 1200°C. About 350 g of particles in the size range of 90–212  $\mu\text{m}$  were used in the bench-scale reactor with sulphur-free kerosene as fuel.

A freeze-granulated material similar to M4MZ-1200 has been investigated previously in both a batch fluidized-bed reactor [67] and a bench-scale reactor with continuous particle circulation [68], using a syngas and a natural gas as fuel. In these experiments, the particles showed high fuel conversion and no issues were reported regarding fluidization, agglomeration or dust formation.

## 2.5.5 Synthetic Copper-based Materials

Different copper-based particles have been used in earlier studies with generally very promising results [21, 69–74]. Copper-based oxygen carriers are known to have good conversion capabilities for solid fuels, which can be attributed by the so called CLOU effect, i.e. the release of gas-phase oxygen in the fuel reactor. Due to the rather low melting point of metallic copper, which can be formed during reduction, high temperatures sometimes cause agglomeration of the oxygen-carrier particles.

### 20 wt% Copper Oxide on Zirconia

The copper-based material C2Z-1050 was produced following the same principle as for the manganese-based material. It consists of an active part, 20 wt% CuO, and an inert part, 80 wt%  $\text{ZrO}_2$ , and was produced through spray-drying with subsequent calcination at 1050°C. The particles were supplied by VITO NV in Mol, Belgium.

The copper-based oxygen carrier C2Z-1050 was used for experiments in the bench-scale reactor with sulphur-free and sulphurous kerosene as fuel. For both fuels, 310 g of particles in the size range of 90–250  $\mu\text{m}$  were used.

### 40 wt% Copper Oxide on Magnesium Aluminate and Titanium Dioxide

The second copper-based material, C4MA4T2-1000, consisted of 40 wt% copper(II) oxide (CuO), 40 wt% magnesium aluminate ( $\text{MgAl}_2\text{O}_4$ ) and 20 wt% titanium dioxide ( $\text{TiO}_2$ ). It was produced by VITO NV in Mol, Belgium, through spray-drying and subsequent calcination at 1000°C. In an extensive study, 27 different oxygen carriers were compared, all with 40 wt% copper oxide on different inert supports and different calcination temperatures [75].

In that study, the material used here was found to be both reactive and resistant to attrition. C4MA4T2-1000 was tested in the bench-scale reactor with sulphur-free kerosene.

### 2.5.6 Manganese Ore

The manganese ore tested, originates from the Buritirama mine in Brazil and contained about 38 wt% of elemental manganese. Other components found in an elemental analysis were 3.9 wt% of aluminium, 2.9 wt% of iron and less than 1 wt% of manganese and zinc. The balance was mainly oxygen and silica as well as smaller amounts of potassium and barium [63]. The ore was ground and sieved to the desired particle size before it could be used as an oxygen carrier. Because of its mineral origin and the small amount of processing necessary, an oxygen carrier based on manganese ore is rather cheap. Prior to the experiments in the bench-scale reactor, the oxygen carrier was used in a pilot-scale unit with petroleum coke as fuel for about 10 h [63]. About 350 g of the used oxygen carrier in the size range of 125–180  $\mu\text{m}$  was used for the experiments in the bench-scale unit.

### 2.5.7 Synthetic Calcium Manganite-based Material

The material based on calcium manganite is of perovskite structure and has the nominal chemical composition  $\text{CaMn}_{0.9}\text{Mg}_{0.1}\text{O}_{3-\delta}$ . The particles were produced by VITO NV in Mol, Belgium, through spray-drying and subsequent calcination at 1300°C for 4 h. This oxygen carrier has CLOU properties, cf. Section 1.1.1.

The calcium manganite-based material was used prior to the experiments described here for tests in a batch fluidized-bed reactor with methane and a syngas as fuel [76], and for an experiment series with a sulphur-free natural gas as fuel [77, 78]. During the latter, fuel was added for 55 h and the particles did not show any signs of chemical degradation. Complete conversion of fuel to  $\text{CO}_2$  and  $\text{H}_2\text{O}$  could be achieved. Furthermore, the amount of fines produced was very low, which indicates a long lifetime. This high resistance to attrition could be confirmed by a test performed in the attrition test-rig [79]. On the basis of these positive characteristics, the material was chosen to establish a proof-of-concept with fuel oil 1 in the pilot-scale unit.

## 2.6 Experiments Performed

### 2.6.1 Syngas Experiments

Ilmenite oxygen carrier was tested with syngas as fuel during 85 h of fuel operation. The syngas used here consisted of 50 vol% hydrogen and 50 vol% of carbon monoxide. Both of these components are important intermediate products when oxidizing solid or liquid fuels. Experiments were carried out at a temperature of 750–950°C and a fuel flow corresponding

---

to 100–340  $W_{th}$ . The initial solids inventory was 270 g but was reduced to 135 g after 31 h of fuel operation in order to study the effect of bed mass. During the last 27 h of fuel operation, steam was added to the fuel, which increased the hydrogen-to-carbon molar ratio from 2 to 2.8.

## 2.6.2 Kerosene Experiments

### Sulphur-free Kerosene

Six different oxygen-carrier materials were tested with a sulphur-free kerosene as fuel under chemical-looping combustion conditions. The total fuel operation time was about 152 h. Table 2.3 gives an overview of the experiments conducted during this test campaign and shows the main experimental parameters. The proof-of-concept was established with the nickel-based material N4MZ-1400. This material was also used during 20 h of chemical-looping reforming experiments with sulphur-free kerosene. Since the focus of this thesis lies on chemical-looping combustion, the reforming tests are not included here. Further details and results can be found in Paper II [15].

**Table 2.3:** Summary of the main experimental parameters for different oxygen-carrier materials used for chemical-looping combustion with sulphur-free kerosene

Experimental parameter	Unit	Oxygen-carrier material					
		Ni on Mg-ZrO <sub>2</sub>	Ilmenite (NOR)	Mn on Mg-ZrO <sub>2</sub>	Cu on ZrO <sub>2</sub>	Cu on MgAl <sub>2</sub> O <sub>4</sub> /TiO <sub>2</sub>	Mn ore (BRA)
Fuel power	W <sub>th</sub>	143-572	143-572	143-458	143-286	143-458	143-286
Fuel flow	ml <sub>liq</sub> /min	0.25-1.00	0.25-1.00	0.25-0.80	0.25-0.50	0.25-0.80	0.25-0.50
Steam flow	ml <sub>liq</sub> /min	0.75	0.75	0.75	0.75	0.75	0.75
Hydrogen-to-carbon ratio	mol/mol	3.3-7.7	3.3-7.7	3.7-7.7	4.8-7.7	3.7-7.7	4.8-7.7
Fuel reactor temperature	°C	750-900	750-950	800-950	650-900	850-900	900
Fuel operation time	h	34	41	17	45	11	4
Initial solid inventory	g	250	380	350	310	360	350
Bed mass in fuel reactor <sup>†</sup>	g	80	110	90	80	95	95
Bed height in fuel reactor (fluidized) <sup>†</sup>	mm	30	115	100	100	100	105
Superficial gas velocity in riser	m/s	0.80-0.92	0.80-0.96	0.73-1.08	0.72-0.92	0.66-0.92	0.80

<sup>†</sup>theoretic value

---

## Sulphurous Kerosene

After the test campaign with sulphur-free kerosene, the most promising oxygen-carrier materials were selected and further tested with a sulphurous kerosene. The materials selected were the mineral material ilmenite and the synthetic, copper-based material C2Z-1050. The scheme of this test campaign was that reference tests with sulphur-free kerosene were conducted before and after the main experiments with sulphurous kerosene. These two reference tests were then compared with each other in order to determine whether fuel conversion had changed during the experiments with sulphurous kerosene. A total of 65 h of fuel operation with both types of kerosene was conducted during this test campaign. The main experimental parameters are shown in Table 2.4.

**Table 2.4:** Summary of the main experimental parameters for different oxygen-carrier materials used for chemical-looping combustion with sulphurous kerosene

Experimental parameter	Unit	Oxygen-carrier material	
		Ilmenite (NOR)	Cu on ZrO <sub>2</sub>
Fuel power	W <sub>th</sub>	100-400	100-200
Fuel flow	ml <sub>liq</sub> /min	0.16-0.65	0.16-0.33
Steam flow	ml <sub>liq</sub> /min	0.75	0.75
Hydrogen-to-carbon ratio	mol/mol	3.9-10.1	6.0-10.1
Fuel reactor temperature	°C	850-950	750-900
Fuel operation time	h	30(+9) <sup>†</sup>	21(+5) <sup>†</sup>
Initial solid inventory	g	380	310
Bed mass in fuel reactor <sup>‡</sup>	g	110	85
Bed height in fuel reactor (fluidized) <sup>‡</sup>	mm	115	105
Superficial gas velocity in riser	m/s	0.88-0.96	0.80-0.92

<sup>†</sup>The parenthesized values are fuel operation times with sulphur-free kerosene that are not included in Table 2.3.

<sup>‡</sup>theoretic value

### 2.6.3 Fuel Oil Experiments

Two different oxygen-carriers materials were investigated during the test campaign with fuel oil 1 in the pilot-scale reactor. A proof-of-concept was established with the calcium manganite-based material CaMn<sub>0.9</sub>Mg<sub>0.1</sub>O<sub>3-δ</sub>. The goal of this study was to check the functionality of the fuel injection system and to gauge to what extent the fuel is converted in the fuel reactor. Two experiments were performed with 38 min and 30 min of fuel injection, respectively. The data evaluation of these experiments is limited, because neither flame ionization detector (FID) nor gas chromatograph (GC) were online. The fuel-reactor temperature was about 900°C. The fuel flow was estimated based on a calibration of the fuel injection system at room temperature and atmospheric pressure.

For the long-term testing, the ilmenite oxygen carrier was used. The goal during this experimental campaign was to test particle integrity and investigate the effect of important parameters on fuel conversion. Initially, the fuel flow was estimated based on a calibration of the fuel injection system at room temperature and atmospheric pressure. Later, during the main part of the experiments, the fuel flow was measured based on weight change of the fuel tank over time. Nine days of experiments with successful fuel injection were performed and a total fuel injection time of 67 h was achieved. The total time of hot operation, i.e. at more than 600°C, was about 204 h. The experimental parameters of this test campaign are summarized in Table 2.5.

**Table 2.5:** Summary of the main experimental parameters for different oxygen-carrier materials used for chemical-looping combustion with fuel oil 1

Experimental parameter	Unit	Oxygen-carrier material	
		CaMn <sub>0.9</sub> Mg <sub>0.1</sub> O <sub>3-<math>\delta</math></sub>	Ilmenite (NOR)
Fuel power	kW <sub>th</sub>	≈ 6	3.9–6
Fuel flow	ml <sub>liq</sub> /min	≈ 10	6.6–10
Steam flow	ml <sub>liq</sub> /min	25.5–30.5	4.0–38.0
Hydrogen-to-carbon ratio	mol/mol	6.6–7.5	2.9–12.0
Fuel reactor temperature	°C	850–900	900–1050
Fuel operation time	h	1	67
Initial solid inventory	kg	≈ 20	22–24
Bed mass in fuel reactor	kg	10.3 <sup>†</sup>	8.4 <sup>‡</sup>
Bed height in fuel reactor (fluidized)	mm	275	275
Superficial gas velocity in riser	m/s	2.7–3.4	2.6–3.6

<sup>†</sup>theoretic value

<sup>‡</sup>measured value

## 2.6.4 Vacuum Residue Experiments

After the experimental campaign with fuel oil 1, the fuel injection system was modified and adapted to heavier fuels, cf. Section 2.3.2. Despite of different modifications, continuous injection of fuel could not be achieved. On several attempts, fuel could be injected for a maximum of 57 min, before the injection system was blocked as a result of fuel fouling. On six attempts, and for a total of about 4 h, two different blends of vacuum residue and fuel oil 1 were injected for 16–57 min. The fuel injection periods were short and only few measurement points of the weight of the fuel tank were retrieved. This, in turn, resulted in a poor judgement on the actual fuel flow to the fuel reactor, in contrast to the long-term tests with fuel oil 1. The experimental settings were similar to those with fuel oil 1. About 22 kg of ilmenite particles were in the reactor system, out of which about 8.4 kg were in fuel reactor. The temperature in the fuel reactor was 850–950°C. A higher steam flow than with fuel oil 1 was used, i.e. 24–30 ml<sub>liq</sub>/min, due to increased cooling of the injection system.

---

The fuel flow was approximately 7.0–9.0 ml<sub>liq</sub>/min (4.5–5.6 kW<sub>th</sub>) for both fuel blends. The resulting hydrogen-to-carbon ratio in the fuel reactor was between 6.6 and 8.1.



---

## 3 Results and Discussion

---

### 3.1 Syngas Experiments

With ilmenite oxygen carrier, full conversion of the syngas to  $\text{CO}_2$  and  $\text{H}_2\text{O}$  was achieved at  $900^\circ\text{C}$  and with a fuel flow that corresponds to about  $190 \text{ W}_{\text{th}}$ . For those conditions, where the conversion of fuel was incomplete, the ilmenite showed a higher reactivity with  $\text{H}_2$  as compared to  $\text{CO}$ . A clear change in the particle structure was observed together with an improvement in fuel conversion during the first hours of fuel operation. After this initial period, fuel conversion did not change considerably over the course of 85 h of fuel operation. The particles were found to be suitable for long-term operation.

More detailed results and discussion can be found in Paper I [49].

### 3.2 Kerosene Experiments

#### 3.2.1 Sulphur-free Kerosene

The evaluation of the combustion process with liquid fuel is based on the quantification of different carbon fractions at the gas outlet of the fuel reactor, which were calculated according to Equations (1)–(4) and are explained in Table 3.1. The sum of these carbon fractions was normalized to one, which means that a possible leakage of fuel carbon to the air reactor was not taken into account. Carbon leakage can occur through two different mechanisms and is likely a combination of both. First, coke could be formed in the fuel reactor and transported into the air reactor. This leakage path is mostly oxygen carrier-specific but could be influenced by the reactor-specific residence time of the coke in the fuel reactor. Second, gaseous reactants could leak from the fuel reactor to the air reactor. This leakage path is mainly reactor-specific but can be related to the oxygen-carrier particles. Experiments with ilmenite oxygen carrier were carried out in both the bench-scale reactor and the pilot-scale reactor. During the evaluation, it was found that the carbon-leakage behaviour differed significantly between the two reactors used. Whereas carbon leakage with ilmenite oxygen carrier and kerosene in the bench-scale reactor was high, up to 11 mol%, it was low in the pilot-scale unit with fuel oil 1 as fuel, and never above 2 mol%. This means that carbon leakage for ilmenite oxygen carrier seems to depend mostly on the reactor

design rather than on the oxygen-carrier material. Consequently, the evaluation of the carbon species in the fuel reactor, according to Equations (1)–(4), was chosen to evaluate the influence of the oxygen-carrier material on the conversion of fuel. In the first publications with kerosene as fuel, i.e. Papers II and III [15, 34], a carbon balance was drawn around the whole reactor system, i.e. air reactor and fuel reactor. Later, in Papers IV and V [35, 36], the focus of the evaluation was on the carbon fractions in the fuel reactor.

$$\gamma_{\text{CO}_2} = \frac{\dot{n}_{\text{CO}_2,\text{FR}}}{\dot{n}_{\text{CO}_2,\text{FR}} + \dot{n}_{\text{CO},\text{FR}} + \sum (x \cdot \dot{n}_{\text{C}_x\text{H}_y\text{O}_z,\text{FR}})} \quad (1)$$

$$f_{\text{CO}} = \frac{\dot{n}_{\text{CO},\text{FR}}}{\dot{n}_{\text{CO}_2,\text{FR}} + \dot{n}_{\text{CO},\text{FR}} + \sum (x \cdot \dot{n}_{\text{C}_x\text{H}_y\text{O}_z,\text{FR}})} \quad (2)$$

$$f_{\text{CH}_4} = \frac{\dot{n}_{\text{CH}_4,\text{FR}}}{\dot{n}_{\text{CO}_2,\text{FR}} + \dot{n}_{\text{CO},\text{FR}} + \sum (x \cdot \dot{n}_{\text{C}_x\text{H}_y\text{O}_z,\text{FR}})} \quad (3)$$

$$f_{\text{CHO}} = \frac{\sum (x \cdot \dot{n}_{\text{C}_x\text{H}_y\text{O}_z,\text{FR}}) - \dot{n}_{\text{CH}_4,\text{FR}}}{\dot{n}_{\text{CO}_2,\text{FR}} + \dot{n}_{\text{CO},\text{FR}} + \sum (x \cdot \dot{n}_{\text{C}_x\text{H}_y\text{O}_z,\text{FR}})} \quad (4)$$

**Table 3.1:** Groups of carbon fractions as used in evaluation

Carbon fraction	Symbol	Explanation
CO <sub>2</sub>	$\gamma_{\text{CO}_2}$	The fraction of CO <sub>2</sub> of the total carbon in the exhaust gases of the fuel reactor is called the CO <sub>2</sub> yield. A special denotation, $\gamma$ instead of $f$ , is chosen to differentiate CO <sub>2</sub> as desired oxidation product from other carbon species CO, CH <sub>4</sub> and C <sub>x</sub> H <sub>y</sub> O <sub>z</sub> .
CO	$f_{\text{CO}}$	CO is an intermediate reaction product. It is formed when hydrocarbons are fully reformed but only partially oxidized.
CH <sub>4</sub>	$f_{\text{CH}_4}$	CH <sub>4</sub> is a common product during the conversion process and may be an intermediate species towards CO <sub>2</sub> and H <sub>2</sub> O.
C <sub>x</sub> H <sub>y</sub> O <sub>z</sub>	$f_{\text{CHO}}$	Organic compounds, which include hydrocarbons C <sub>m</sub> H <sub>n</sub> with exception of CH <sub>4</sub> , originate from fuel molecules that are partially or not at all reformed. Partially reformed molecules can be partially oxidized.

The CO<sub>2</sub> yield,  $\gamma_{\text{CO}_2}$ , is a single valued measure of how much carbon in the fuel reactor is fully converted into CO<sub>2</sub>, without differentiating between intermediate conversion products. It can be used to compare the performance of different oxygen-carrier materials.

Selected results of the experimental campaign with different oxygen-carrier materials and sulphur-free kerosene as fuel are presented in Figure 3.1. The figure shows carbon fractions, which includes the CO<sub>2</sub> yield, for different oxygen-carrier materials at varied temperature and a fuel flow corresponding to 143 W<sub>th</sub>. No results are shown for the copper-based material C4MA4T2-1000 and the manganese ore. The results with C4MA4T2-1000 are very similar to those of C2Z-1050, except that C4MA4T2-1000 could be tested with higher fuel

flows, which was because of its higher copper content. Fuel conversion with the manganese ore was very low and, therefore, only very few experimental parameters were tested. The results of the oxygen-carrier materials shown, indicate different behaviours with respect to fuel conversion.

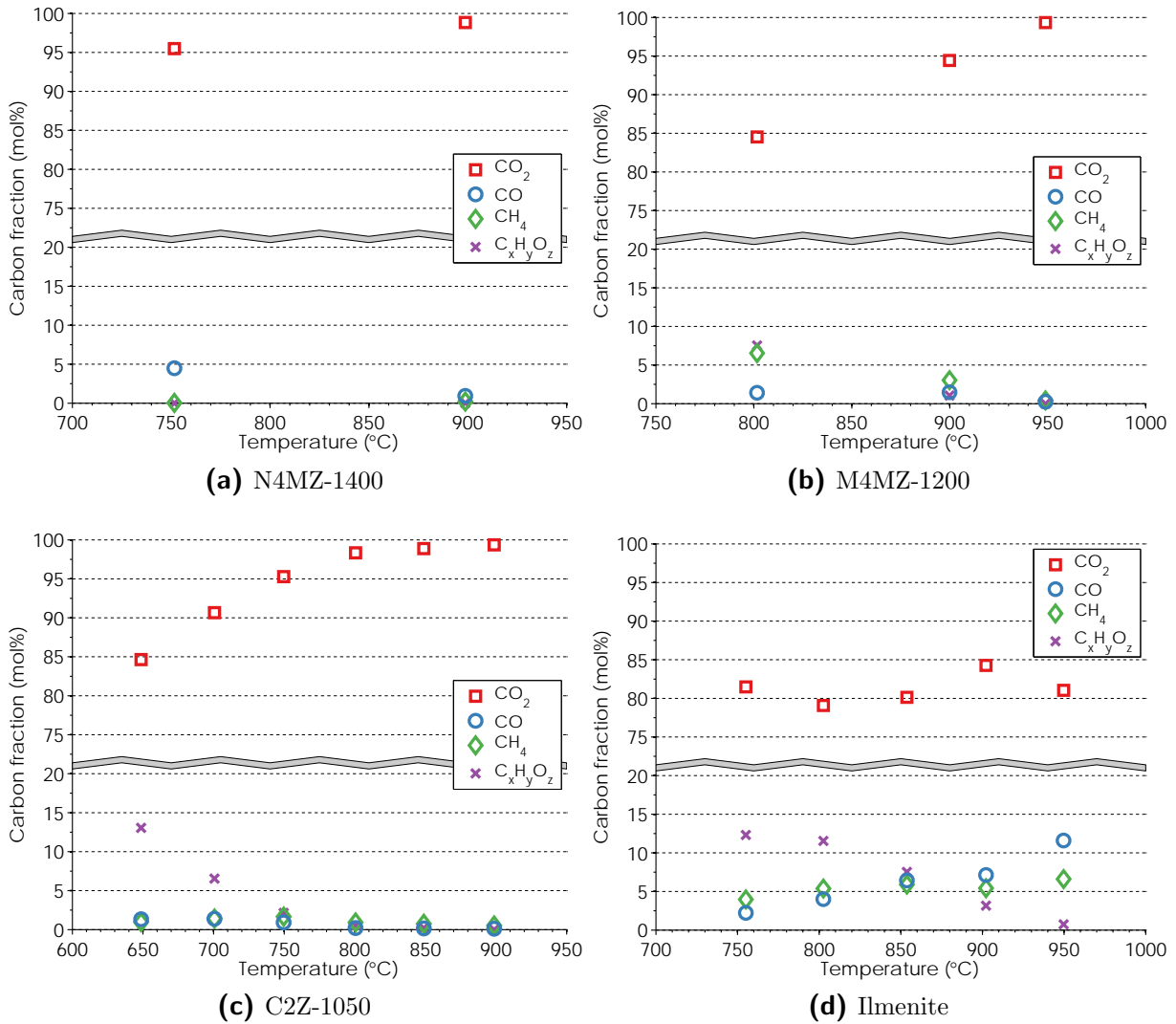


**Figure 3.1:** Carbon fractions and CO<sub>2</sub> yield for different oxygen carriers at varied temperatures with a flow of 0.25 ml<sub>liq</sub>/min (143 W<sub>th</sub>) of sulphur-free kerosene

Fuel conversion with N4MZ-1400, see Figure 3.1a, was very good and nearly complete. The CO<sub>2</sub> yield was above 95 mol% at all times. The unconverted gases were mainly CO and H<sub>2</sub>, with H<sub>2</sub> not being shown here. The high but incomplete gas yield of fuel to CO<sub>2</sub> can be ascribed to thermodynamic limitations of nickel-based oxygen carriers. No noteworthy concentrations of CH<sub>4</sub> or any other organic compounds were observed. This is likely a result of catalytic properties of nickel-based materials, which promote decomposition of hydrocarbons. The nickel-based oxygen carrier was used to establish a proof-of-concept in the bench-scale unit with sulphur-free kerosene. Freeze-granulation produced regular

solid and spherical particles but large-scale production with this technique is probably not technically feasible. Therefore, and because of the general disadvantages connected with nickel-based materials, see Section 2.5.2, this material was not considered to be a convenient oxygen-carrier material in a larger scale. For a more detailed discussion, see Paper II [15].

Fuel conversion with M4MZ-1200 clearly increased with higher temperatures, as can be seen in Figure 3.1b. The amount of CO is low for all temperatures, whereas methane and other organic compounds were detected at temperatures below 950°C. Fuel conversion was nearly complete at 950°C. Over the course of the experiments, nearly the whole batch of M4MZ-1200 disintegrated to fines. This problem with mechanical stability is believed to be connected to the support material, ZrO<sub>2</sub>, and might be overcome if either a different support was used or if high temperatures, including those during calcination, were avoided. For this project, however, this material was not considered for further testing. More detailed results can be found in Paper III [34].

Chemical-looping combustion experiments with C2Z-1050 were conducted at lower temperatures than with other oxygen carriers. This was due to the low melting temperature of copper in addition to the high partial pressure of the metal-oxide system CuO/Cu<sub>2</sub>O at combustion temperatures. In order to be able to oxidize the material at a reasonable concentration of oxygen, e.g. 5 vol%, it is necessary to limit operation to around 950°C. The fuel conversion achieved, see Figure 3.1c, was higher than for the other oxygen carriers in this study, including that of nickel-based N4MZ-1400. The CO<sub>2</sub> yield was above 84 mol% for all temperatures investigated and higher than 95 mol% at 750°C or above. The amount of organic compounds clearly decreases at higher temperatures and the dry-gas concentrations of CO and CH<sub>4</sub> were below 1 vol% for the entire temperature interval tested. The dry-gas concentration of H<sub>2</sub> was as high as 4 vol% at the lowest temperature tested, i.e. 650°C. This comparatively high value can be attributed to the water-gas shift reaction, which favours a shift from CO/H<sub>2</sub>O to CO<sub>2</sub>/H<sub>2</sub> at temperatures below 820°C. The variation of fuel flow with this copper-based material was limited by two factors: the low amount of active material, which was about 20%, and the circulation rates that can be achieved in the bench-scale reactor. Hence, the fuel flow could not be increased above 143 W<sub>th</sub>. At this fuel flow rate, however, C2Z-1050 reached the highest CO<sub>2</sub> yield of all the oxygen-carrier materials tested. The high degrees of conversion reached with both copper-based materials, C2Z-1050 and C4MA4T2-1000, can likely be attributed to the uncoupling effect of the oxygen carrier, i.e. the release of oxygen to the gas phase as a function of temperature and partial pressure of oxygen. Thus, the main mechanism of fuel conversion is likely different for this material, as compared to the other evaluated oxides. The material C2Z-1050 was relatively stable in the bench-scale unit. More details can be found in Paper III [34].

Fuel conversion with the copper-based material C4ZMA4T2-1000 was very high and similar to that of afore-mentioned copper-based material C2Z-1050. However, the production of fines was high and the material was not considered for further testing. It should be mentioned that the two support materials have been found to form MgTi<sub>2</sub>O<sub>5</sub> during chemical-looping combustion tests at 950°C [75]. This type of phase transformation can

---

cause structural instabilities in oxygen carriers and might have been avoided at lower temperatures.

Fuel conversion with the mineral ilmenite oxygen carrier, which is shown in Figure 3.1d, differs from fuel conversion with the other oxygen carriers tested. It is clearly lower, i.e. the amounts unconverted  $H_2$ , CO,  $CH_4$  and other organic compounds are higher, and the  $CO_2$  yield does not seem to increase with higher temperatures. The following observations were made with respect to these experiments.

- The amount of carbon in the form of organic compounds decreases at higher temperatures.
- The amount of carbon in the form of  $CH_4$  seems to be rather constant.
- The carbon fraction of CO increases at higher temperatures, as organic compounds are broken down and partially oxidized.

These observations in the temperature interval of 750–950°C could be explained by two parallel fuel conversion mechanisms. (1) Thermal decomposition of hydrocarbons, which increases at higher temperatures. Methane seems to be a rather stable intermediate product on the reaction path from hydrocarbons to  $CO_2$ . (2) The conversion of CO to  $CO_2$  also increases with temperature but slower than the thermal decomposition and consequently the fraction of CO in the flue gases of the fuel reactor increases with temperature. Unfortunately, temperatures higher than 950°C were not tested in this campaign. Following this logic, however, the fractions of both CO and  $CH_4$  should decrease at temperatures above 950°C, whereas the  $CO_2$  yield should increase. This speculation is confirmed by the results in Section 3.3. As a conclusion, the use of ilmenite oxygen carrier in combination with liquid fuel seems most feasible at temperatures above 950°C.

The highest  $CO_2$  yield was clearly reached with both copper-based materials and the nickel-based material, see Figure 3.2. Although it was possible to achieve almost full conversion with the manganese-based material, a higher temperature than for the afore-mentioned oxygen carriers was required. The  $CO_2$  yield for the ilmenite oxygen carrier does not seem to change much in the temperature interval tested here but is expected to increase for temperatures above 950°C.

The summary in Table 3.2 is an attempt to condense the findings from the test campaign with sulphur-free kerosene into one simple comparison. On the basis of this comparison, two oxygen-carrier materials were selected for further testing with sulphurous kerosene and possible testing in the pilot-scale reactor with fuel oil 1. The nickel-based oxygen carrier was only used to establish a proof-of-concept and was, due to its thermodynamic limitations, its toxicity and its vulnerability to sulphur poisoning, never meant for further testing. The ilmenite oxygen carrier has generally good properties, except for fuel conversion. However, fuel conversion is believed to improve at temperatures higher than 950°C. The low lifetime of the manganese-based oxygen carrier makes it unfeasible for use in larger circulating fluidized-bed reactors, where the mechanical stress on the particles is significantly higher than in the bench-scale reactor. The copper-based material C2Z-1050 worked generally well but its limited lifetime might produce problems when used in a larger test reactor.

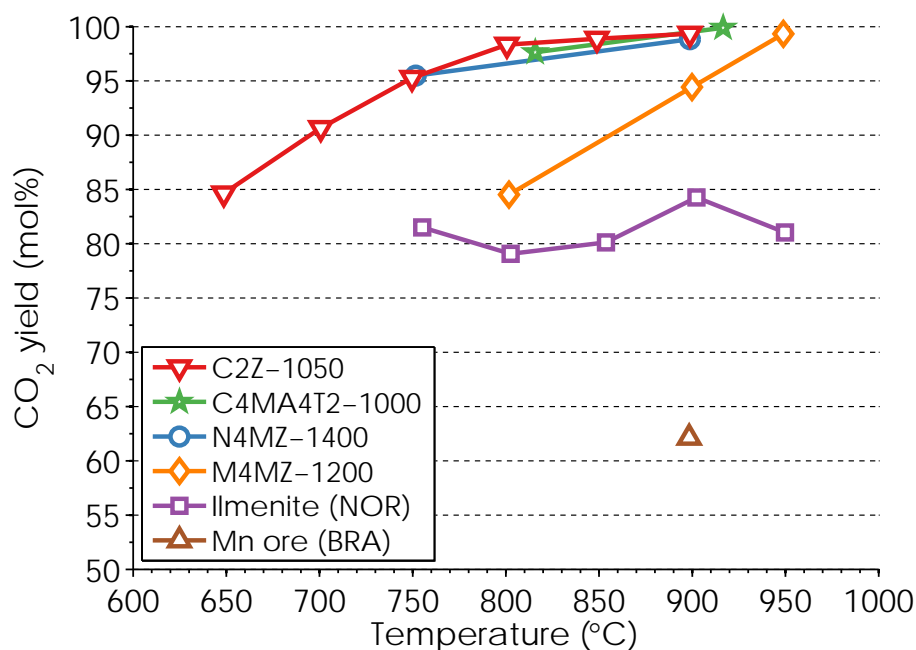


**Figure 3.2:** Comparison of CO<sub>2</sub> yield for different oxygen carriers at varied temperatures with a flow of 0.25 ml<sub>liq</sub>/min (144 W<sub>th</sub>) of sulphur-free kerosene

Also, agglomeration of the particles can be a problem if the material is reduced too far in combination with high temperatures. The copper-based material C4MA4T2-1000 performed similarly to the afore-mentioned copper-based oxygen carrier, except that it had a lower lifetime. Therefore, this material was not further tested. Finally, the manganese ore was also excluded from further testing because it achieved the lowest fuel conversion of all oxygen-carrier materials tested. It is not clear whether the reactivity of the used manganese ore was the same as in the fresh material or if it was a result of a deactivation by petroleum coke, which contained ash and a high amount of sulphur.

In the following experimental campaign, ilmenite oxygen carrier and the copper-based material C2Z-1050 are tested with sulphurous kerosene.

### 3.2.2 Sulphurous Kerosene

A detailed analysis of 33 h of operation with ilmenite oxygen carrier and kerosene with and without sulphur was made. There are clear indications that a dramatic increase in reactivity takes place within the first five hours of operation with sulphurous fuel. Reactivity was low during all experiments before these first five hours, whereas all subsequent experiments showed high reactivity. The corresponding data for a fuel input of 144 W<sub>th</sub> is shown in Figure 3.3.

A separate analysis was carried out in a batch fluidized-bed reactor to investigate the change in reactivity of the ilmenite oxygen-carrier particles. Material from the experiments with sulphurous kerosene was compared with freshly activated ilmenite and it was found

**Table 3.2:** Comparison of crucial properties of the oxygen carriers tested with sulphur-free kerosene

Oxygen-carrier material	Fuel conversion	Lifetime	Agglomeration tendency	Estimated costs <sup>†</sup>
Ni on Mg-ZrO <sub>2</sub>	++	-	+	--
Ilmenite (NOR)	-	++	+/-	++
Mn on Mg-ZrO <sub>2</sub>	+	--	+	-
Cu on ZrO <sub>2</sub>	++	+/-	-	-
Cu on MgAl <sub>2</sub> O <sub>4</sub> /TiO <sub>2</sub>	++	-	-	-
Mn ore (BRA)	--	+	+	+

The evaluation scale used in this table goes from “++”, which is a most favourable property, to “--”, which is a least favourable property.

<sup>†</sup>Freeze-granulated particles receive a “-” rating, spray-dried particles receive a “-” rating and minerals receive a “+” or “++” rating, depending on their relative market price.

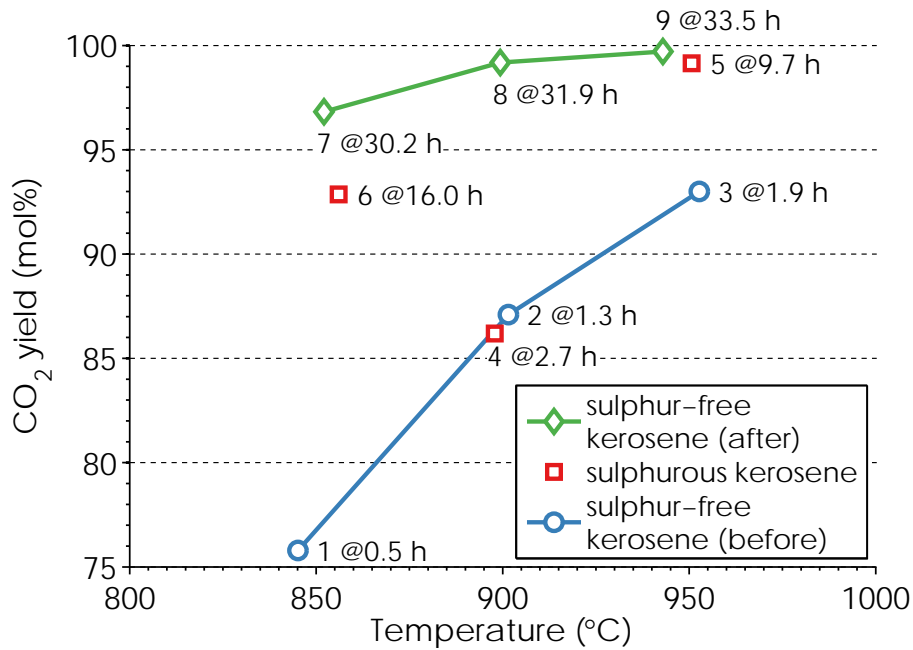


**Figure 3.3:** Comparison of experiments with ilmenite oxygen carrier and sulphur-free and sulphurous kerosene. Reference experiments with sulphur-free kerosene were performed both before and after the main tests with sulphurous kerosene. A constant fuel flow equivalent to  $144 W_{th}$  was used for both types of kerosene. The order in which the experiments were performed is shown together with the cumulative fuel operation time.

that the conversion of methane is much higher with the used ilmenite than with the freshly activated ilmenite. This confirms that the oxygen-carrier material was activated in some way during the experiments with sulphur.

Experiments similar to the afore-mentioned ones were performed with the copper-based oxygen carrier C2Z-1050 and sulphur-free and sulphurous kerosene. Fuel conversion during the initial reference experiment with sulphur-free kerosene, see Figure 3.4, was similar to the conversion achieved in the original test campaign with sulphur-free kerosene, i.e. Figure 3.1c. While the conversion of sulphurous kerosene was somewhat lower than that of the initial reference experiment, the degree of conversion reached during the final reference experiment was on a much lower level, which indicates a deactivation of particle reactivity. Parallel with the decrease in fuel conversion, it was observed that the amount of oxygen-carrier particles that degraded to fines and was elutriated from the reactor was much higher than during the experiment campaign with sulphur-free kerosene. The reason for the increased disintegration is unknown but it is likely that it is also the reason for the decrease in fuel conversion observed.

Since the resistance to attrition of the copper-based material C2Z-1050 seems to vary significantly, it was decided not to use this material in the pilot-scale reactor. This decision was supported by attrition tests that were performed on both unused and used particles. These tests showed that the resistance to attrition was low for the fresh material and still lower for the material used for the experimental campaign with sulphur-free fuel. The attrition test-rig that was used for these tests gives an indication of mechanical resistance in conditions similar to those in larger circulating fluidized-bed units. The mechanical wear of particles in larger units, like the pilot-scale unit described in Section 2.1.2, is usually much higher than in the bench-scale unit. This is mainly due to the much higher gas velocities in the grid-jet region in the bottom of the riser and due to wall friction in the cyclone. More details about the attrition test unit and tests performed on different oxygen-carrier materials can be found in [79].

It could be speculated that the reduced attrition resistance of C2Z-1050 in the presence of sulphur is the result of an additional phase change. Jerndal et al. showed that copper sulphate,  $\text{Cu}_2\text{SO}_4$ , and copper sulphide,  $\text{Cu}_2\text{S}$ , can theoretically be formed at high gas yields of the fuel but only at very high concentrations of sulphur-containing gases [80]. However, Keller et al. investigated the interaction of mineral matter with different oxygen-carrier materials and found that  $\text{Cu}_2\text{S}$  was formed when a copper-based material was mixed with pyrite,  $\text{FeS}_2$ , and reduced with hydrogen at  $900^\circ\text{C}$  for 9 h [81]. In the experiments with sulphurous kerosene, the partial pressure of steam was high due the steam added in the injection system. The gas yields obtained were very high as well. Consequently, such highly reducing conditions are unlikely to have occurred overall in the reactor. However, conditions that promoted the formation of sulphates or sulphides might have occurred locally in the fuel reactor and caused a phase change, which, in turn, induced mechanical stress in the material.

### 3.3 Fuel Oil Experiments

The experiments in the pilot-scale unit were evaluated somewhat differently than the experiments in the bench-scale reactor. The main evaluation method was still the quantification

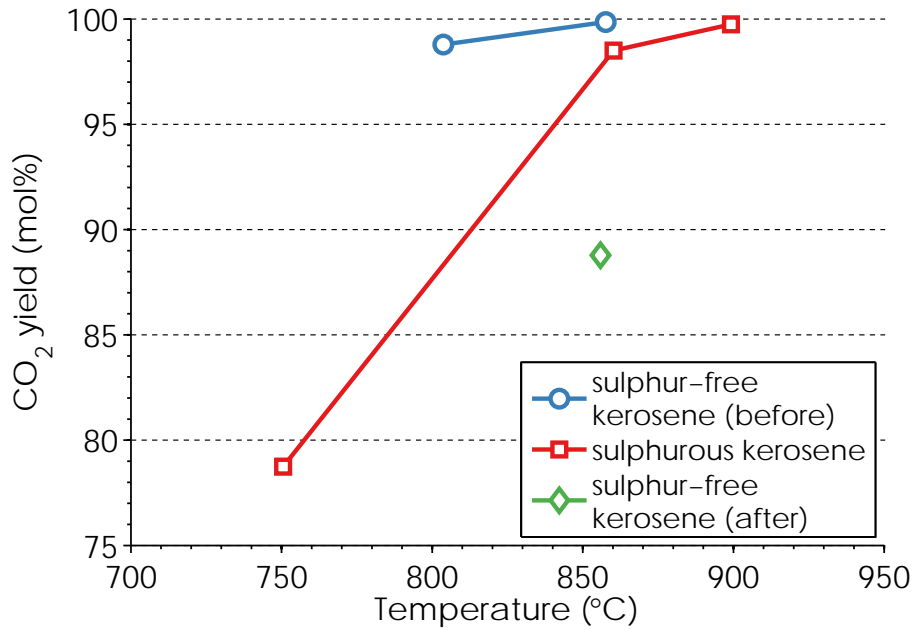


**Figure 3.4:** Comparison of experiments with copper-based oxygen carrier C2Z-1050 and sulphur-free and sulphurous kerosene. Reference experiments with sulphur-free kerosene were performed both before and after the main tests with sulphurous kerosene. A constant fuel flow equivalent to  $144 W_{th}$  was used for both types of kerosene.

of the different carbon fractions in the flue gas of the fuel reactor, cf. Equations (1)–(4) and Table 3.1. In addition, the circulation of solids, which allows for the comparison of different circulating fluidized-bed units, was estimated on the basis of pressure measurements. Gas leakage between air reactor and fuel reactor of the pilot-scale unit does virtually not exist, which facilitates the quantification of both the fuel carbon that leaks into the air reactor and the oxygen that is consumed in the air reactor and transported to the fuel.

The circulation index,  $G'_s$ , is used as a measure of the circulation of solids, and it was calculated according to Equation (5). This equation was adapted to the pilot-scale unit and expresses the circulation as mass flow per area in  $\text{kg}/\text{m}^2\text{s}$  with the cross-sectional area of the riser as reference. It represents the gross amount of particles in motion, i.e. the sum of particles traveling upward and downward, and, hence, it gives an overestimation of the true mass flux of solids. For a pilot-scale chemical-looping reactor similar to the one used here, it was shown that the circulation index is proportional to the true mass flux [82]. In Equation (5),  $\Delta h$  is the vertical difference in height in the middle of the riser over which the pressure drop  $\Delta p$  is measured,  $u_0$  is the superficial gas velocity and  $u_t$  is the terminal velocity of the particles, which was approximated according to [83]. More details about the calculation of the circulation index can be found in [36].

$$G'_s = -\frac{1}{g} \cdot \frac{\Delta p}{\Delta h} \cdot (u_0 - u_t) \quad (5)$$

A simple and straightforward way to evaluate the conversion of fuel is to compare the

amount of oxygen consumed in the air reactor with the stoichiometric amount of oxygen needed for full conversion of fuel to CO<sub>2</sub> and H<sub>2</sub>O. Equation (6) shows how the degree of fuel oxidation,  $\eta_{\text{fuel}}$ , is calculated.

$$\eta_{\text{fuel}} = \frac{\dot{n}_{\text{O}_2, \text{AR}, \text{in}} - \dot{n}_{\text{O}_2, \text{AR}, \text{out}}}{\dot{n}_{\text{O}_2, \text{stoich}}} \quad (6)$$

The significance of Equation (6) strongly depends on the amount of fuel that leaks into the air reactor. If a large amount of fuel leaks into the air reactor, e.g. as coke or reactive gas, oxygen consumption will still be high but at a sacrifice of CO<sub>2</sub> capture efficiency. On the basis of the concentration of CO<sub>2</sub> in the exhaust gases from the air reactor, the fraction of fuel carbon that leaks into the air reactor,  $f_{\text{C}, \text{AR}}$ , was determined according to Equation (7). The flow of CO<sub>2</sub> leaving the air reactor is compensated for the atmospheric concentration of CO<sub>2</sub>, which was approximately 400 ppm during the time of the experiments.

$$f_{\text{C}, \text{AR}} = \frac{\dot{n}_{\text{CO}_2, \text{AR}, \text{out}}}{\dot{n}_{\text{C}, \text{fuel}}} \quad (7)$$

A proof-of-concept for the pilot-scale unit with direct injection of liquid fuel was established with the calcium manganite-based oxygen carrier. During two experiments, the fuel oil was injected for a total of 68 min, and most of the fuel carbon was converted to CO<sub>2</sub>. Average values for oxidation of fuel, circulation index and carbon leakage to the air reactor are shown Table 3.3. The degree of fuel oxidation for both experiments fluctuated between 60% and 85%. No or little organic compounds higher than C<sub>2</sub>H<sub>y</sub>O<sub>z</sub> were present, and the amount of carbon that leaked to the air reactor was very low. Long-term testing with this batch of particles was not feasible, because a large fraction of the particles was in a size range that was too small for the existing cyclone of the pilot-scale reactor. Consequently, particles were elutriated from the system at a high rate. This, however, could be fixed easily, either by adapting the cyclone or by producing a new batch of this material in a larger size range.

**Table 3.3:** Average process values of both proof-of-concept experiments with calcium manganite-based oxygen carrier. The temperatures in air reactor and fuel reactor were 850–900°C and the fuel flow corresponded to roughly 6 kW<sub>th</sub>.

Process value	Unit	Experiment 1	Experiment 2
Degree of fuel oxidation, $\eta_{\text{fuel}}$	%	77	68
Circulation index, $G'_s$	kg/m <sup>2</sup> s	3.0	3.3
Carbon leakage to air reactor, $f_{\text{C}, \text{AR}}$	mol%	0.75 <sup>†</sup>	0.52 <sup>†</sup>
Fuel injection time	min	38	30

<sup>†</sup>The carbon leakage was calculated on the basis of measurements of CO<sub>2</sub> in the air reactor. The average CO<sub>2</sub> concentration was 0.09 vol% (including atmospheric CO<sub>2</sub>) in both experiments.

Some problems were experienced with fouling of fuel, which led to blocking of the fuel injector. Fouling of organic fluids is a known problem and happens through three main

processes: autoxidation, thermal decomposition and polymerization [53]. The problems experienced are believed to have been caused by thermal decomposition of the fuel followed by polymerization. The influence of autoxidation of fuel in the fuel line is believed to be negligible. An increase of the steam flow surrounding the injection nozzle in order to increase cooling solved the problem. Henceforward, the injection system could be used successfully in repeated operation.

After the proof-of-concept was established, long-term experiments were performed with ilmenite oxygen carrier and fuel oil 1. The oxygen carrier was fluidized under hot conditions, i.e. more than 600°C, for about 204 h, out of which 66.6 h were with addition of fuel. During the first experiments with ilmenite oxygen carrier, a fuel flow of about 10 ml<sub>liq</sub>/min (6 kW<sub>th</sub>) was used. Fuel oxidation was low, i.e. below 45% at 900°C and about 65% at 1000°C, and, consequently, the fuel flow was reduced to about 7.2 ml<sub>liq</sub>/min (4 kW<sub>th</sub>).

Figure 3.5 shows the degree of fuel oxidation over the circulation index at different temperatures. Two general trends can be observed here. First, fuel oxidation increases at higher temperatures. Second, increased particle circulation leads almost always to an increased oxidation of fuel. The maximum degree of fuel oxidation is about 87%.

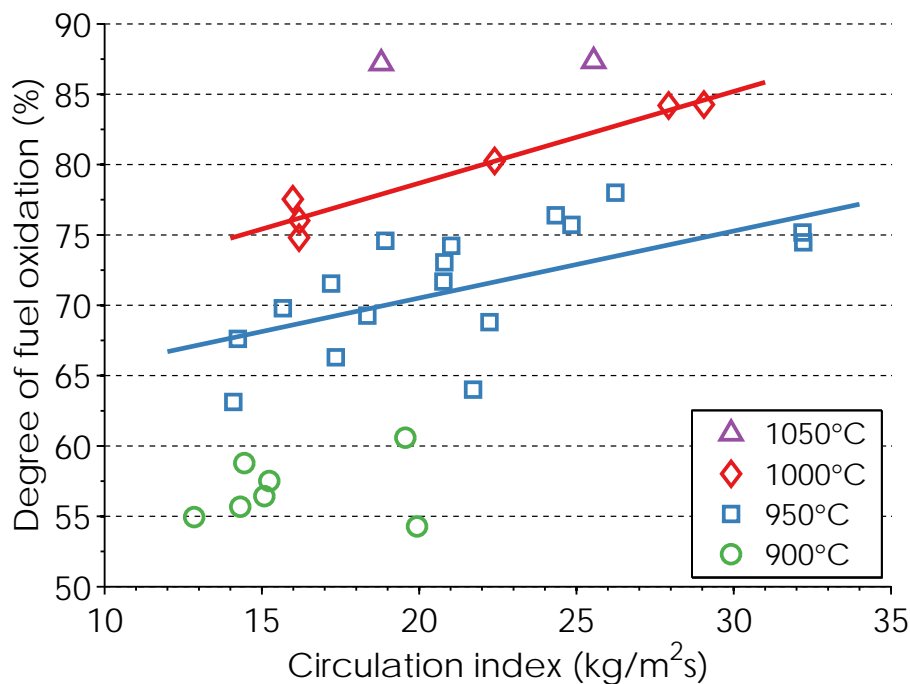


**Figure 3.5:** Degree of fuel oxidation with ilmenite oxygen carrier at varied circulation index and different fuel-reactor temperatures. The fuel flow corresponds to about 4 kW<sub>th</sub>. Each data point depicts average values of one experimental setting, which lasted 20–189 min, and 86 min on average.

The effect of variation of fuel flow is shown in Figure 3.6. Here, the degree of fuel oxidation is shown for fuel flows that correspond to about 4 kW<sub>th</sub> and 6 kW<sub>th</sub>, respectively. A clear increase in degree of oxidation at both increased temperature and decreased fuel flow can

be seen. The difference in fuel oxidation between the two fuel flows tested is about 10 %-points. Reasons for that can be one or a combination of the following:

- Decrease in the contact time between gas and solids due to an increased gas flow in the fuel reactor.
- Higher bypass of combustible gases through gas channels in the fluidized bed of the fuel reactor.
- Reduced reactivity of the oxygen carrier in the fuel reactor.<sup>5</sup>

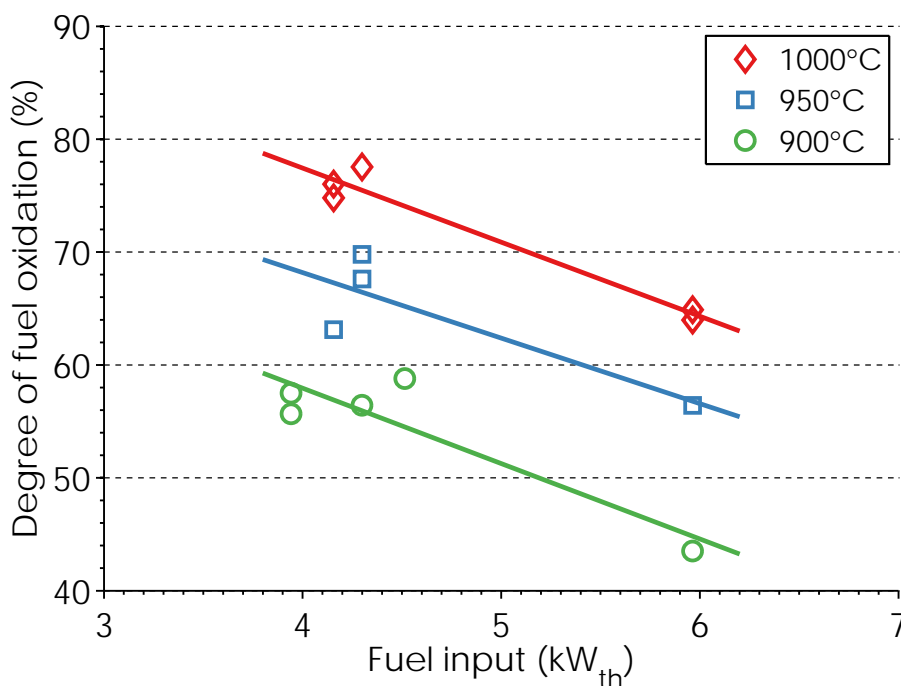


**Figure 3.6:** Degree of fuel oxidation with ilmenite oxygen carrier at varied fuel flow and different fuel-reactor temperatures. The circulation index for all data points shown was similar and 14–17 kg/m<sup>2</sup>s.

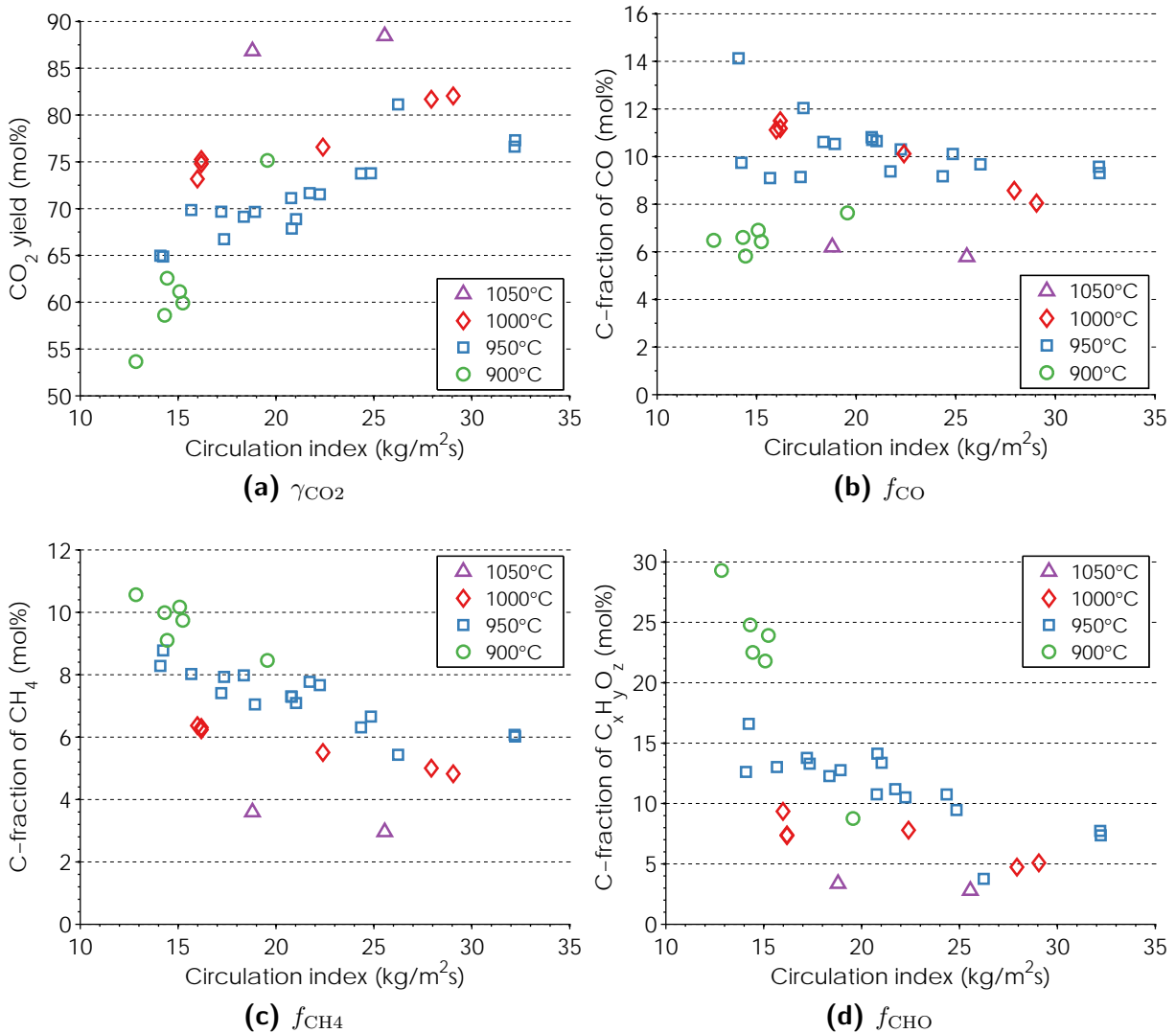
The average leakage of fuel carbon to the air reactor was usually below 1 mol% and never above 2 mol%. This carbon fraction is sensitive to changes in the measured CO<sub>2</sub> concentration. The fact that the CO<sub>2</sub> concentration in the air reactor was very close to the atmospheric concentration of CO<sub>2</sub>, and also close to the lower detection limit of the gas analyzer, adds a certain margin of error to the results. However, it can be said with certainty that carbon leakage to the air reactor was very low and, hence, a very high degree of carbon capture was achieved.

Figure 3.7 shows different carbon fractions in the fuel reactor, i.e. how much of the total carbon in the fuel reactor is in the form of (a) CO<sub>2</sub>, (b) CO, (c) CH<sub>4</sub> and (d) organic

<sup>5</sup>Ilmenite has a decreasing reactivity for conversion of CH<sub>4</sub>, CO and H<sub>2</sub> the more its degree of oxidation is reduced [62, 84, 85].

compounds  $C_xH_yO_z$  not including methane. The following observations can be made in Figure 3.7:

- The  $CO_2$  yield increases at higher temperatures and higher circulation indexes, see Figure 3.7a. The maximum  $CO_2$  yield was about 88 mol%.
- The fraction of organic compounds including  $CH_4$  decreases at higher temperatures and higher circulation indexes, see Figure 3.7c and 3.7d.
- The carbon fraction of CO increases from 900°C to 950°C and decreases from 1000°C to 1050°C, see Figure 3.7b. The CO fractions at 950°C and 1000°C are similar, as well as those at 900°C and 1050°C. Thus, the carbon fraction of CO seems to reach a maximum between 950°C and 1000°C.



**Figure 3.7:** Carbon fractions in the fuel reactor with ilmenite oxygen carrier and fuel oil 1; **(a)**  $\gamma_{CO_2}$  ( $CO_2$ ), **(b)**  $f_{CO}$  ( $CO$ ), **(c)**  $f_{CH_4}$  ( $CH_4$ ) and **(d)**  $f_{CHO}$  (organic compounds except  $CH_4$ ). The fuel flow corresponds to about 4 kW<sub>th</sub>.

The concentration of hydrogen measured was generally proportional to the carbon fraction of CO in Figure 3.7b and varied between 6 vol% and 16 vol%. The concentration of hydrogen decreases at higher circulations of solids and seems to peak between 950°C and 1000°C. With steam used to fluidize the particles in the fuel reactor, the concentration of hydrogen measured was always below, usually about half, the equilibrium concentration predicted by the water–gas shift reaction.

More details about this experimental campaign can be found in Paper V [36].

## 3.4 Vacuum Residue Experiments

Subsequent to the positive results from the campaign with ilmenite oxygen carrier and fuel oil 1, a new test campaign was started, which had the aim of injecting blends of vacuum residue and fuel oil 1. Several successful injections were performed with two different blends, though only for a limited time. A build-up of pressure in the fuel line occurred at varying rates and ultimately led to the abortion of fuel injection after 16–57 min. The same behaviour was experienced during the proof-of-concept experiments with fuel oil 1, cf. Section 3.3. This time, however, cooling of the fuel nozzle could not be increased sufficiently in order to prevent fuel fouling in the injection system completely and, consequently, all experiments ended with blocking of the fuel nozzle. It is believed that heat transfer to the injection system can be reduced sufficiently with an improved design of the injection system, which is discussed in Section 3.4.1.

The first blend tested consisted of 40 wt% vacuum residue and 60 wt% fuel oil 1. This blend is free flowing at room temperature and did not require heating of the fuel line. Four successful injections were performed at 800–900°C. After these tests, a second blend was tested, which contained 80 wt% vacuum residue and 20 wt% fuel oil 1. This blend was clearly thicker than the first one but still free flowing at room temperature. In order to ensure that the blend could flow freely through a filter into the inlet of the fuel pump, the fuel was heated to about 30°C. In that way, two experiments could be performed at 900–950°C. During this campaign, the oxygen carrier was fluidized in hot state for about 132 h and fuel was added for just about 5 h, out of which 1 h was with fuel oil 1.

Figure 3.8 shows the degree of fuel oxidation for the six experiments with blends of vacuum residue and fuel oil 1. Additionally, and as a reference, data points from the experiments with unblended fuel oil 1, cf. Figure 3.5, are shown. Both temperature and circulation index were lower during the experiments with blends of vacuum residue and fuel oil 1, which resulted in a somewhat lower conversion than with pure fuel oil. A general observation, however, is that the degree of fuel oxidation seems to be in line with the data from the test campaign with fuel oil 1. In other words, differences in conversion of fuel between the experiments with different fuel mixes can be attributed to a lower temperature and/or a lower circulation index. The carbon that was detected in the flue gas from the air reactor corresponded to 0.4–2.5 mol% of the total fuel carbon, without following any obvious trends

with respect to temperature and circulation index. This complies in quantity and quality with the carbon leakage behaviour observed during the test campaign with fuel oil 1.

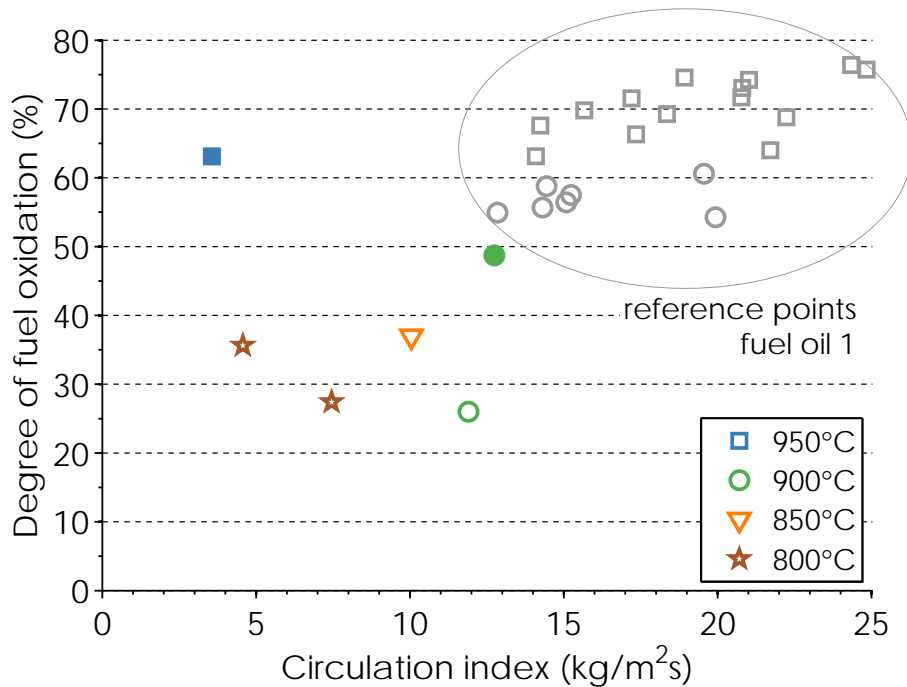


**Figure 3.8:** Degree of fuel oxidation with ilmenite oxygen carrier for different fuel-reactor temperatures. The fuel flow corresponds to 4.5–5.6 kW<sub>th</sub>. The filled markers represent experiments with the 80:20 blend of vacuum residue and fuel oil and the unfilled markers represent experiments with the 40:60 blend. The gray markers are reference points from the experiments with fuel oil 1, cf. Figure 3.5. Each data point depicts average values of one experimental setting, which lasted 16–57 min.

Not all measurement instruments were online during these first tests with blends of vacuum residue and fuel oil 1 and, hence, the data available is limited. Furthermore, the method of determining the fuel flow on the basis of manually logged values has an accuracy, which depends on the number of measurements and the duration of fuel injection, respectively. Another problem with short injection intervals is that a steady state is not necessarily achieved. The transient behaviour of the pilot-scale unit upon fuel injection is usually 10–20 min but can be potentially longer. Despite lacking and uncertain data, and the problems with the injection of fuel, important observations could be made.

Clear differences in conversion of liquid fuel could be observed for different oxygen-carrier materials using the bench-scale reactor. There, ilmenite oxygen carrier achieved clearly lower levels in fuel conversion than most other materials tested. A dramatic and lasting improvement in fuel conversion was observed after at least 3 h of operation with sulphurous kerosene. Here, however, it is not clear whether a similar improvement took place during less than 4 h of operation with vacuum residue and fuel oil 1. It can be expected that the conversion of vacuum residue would be significantly improved if an oxygen-carrier material with CLOU properties was employed. The calcium manganite-based material that was

used for the proof-of-concept experiments with fuel oil 1 achieved promising results but is known to be deactivated in the presence of sulphur [86]. In the same study, Arjmand et al. also found that the presence of both magnesium and titanium as dopants increases the resistance to sulphur deactivation. Hence, a combined manganese material with CLOU properties that has a high resistance to both attrition and deactivation by sulphur seems to be a suitable material for chemical-looping combustion of vacuum residue.

#### 3.4.1 Improvements of the Injection System for Vacuum Residue

In the current injection system, the temperature of the fuel is believed to have exceeded 350°C, which resulted in fouling of the fuel and blocking of the injection system. The main challenges with the injection system, as presented in Section 2.3.2, are the following:

- A fuel is to be introduced close to the center of a bubbling fluidized bed so that it can disperse evenly throughout the cross-section of the fluidized bed.
- The fluidized bed has a temperature of 900°C or more.
- The temperature of the fuel in the injection system must not exceed 350°C in order to avoid fuel fouling there.
- The higher the fuel temperature in the injection nozzle, the lower the viscosity of the fuel and, consequently, the lower the pressure in the fuel line.
- The injection system is small, which makes monitoring of the fuel temperature difficult.

In the injection system, heat that originated from the fluidized bed is transferred to the fuel. The dominating heat transfer mechanisms are radiation (net heat transfer from wall to fuel tube) and convection (from fuel tube to steam and from wall to steam). A reduction of the temperature of the injection system's inner wall will primarily reduce the transfer of radiative heat. Such a reduction in wall temperature could be achieved with a double-walled injection system, i.e. a closed cooling system in addition to the existing open cooling system with steam.

If the distance between the injection system and the fluidized bed, which is the source of thermal radiation, would be increased, the heat transfer to the injection system could be further reduced. However, this might deteriorate the distribution of fuel in the fluidized bed, and consequently, the conversion of fuel.

Figure 3.9 shows a possible design of an improved injection system for vacuum residue, which incorporates the two ideas mentioned above, namely, active cooling of the wall of the injection system and increase of the distance between the fluidized bed and the fuel nozzle. The outer diameter of the injection system is increased from 17.2 mm to 26.7 mm, which is still a reasonable size for a small-scale reactor system, like the one used here. A heat-transfer calculation of the system is recommended in order to assess whether it is necessary to incorporate both measures. Especially the construction of a double-walled injection system with a labyrinth is difficult.

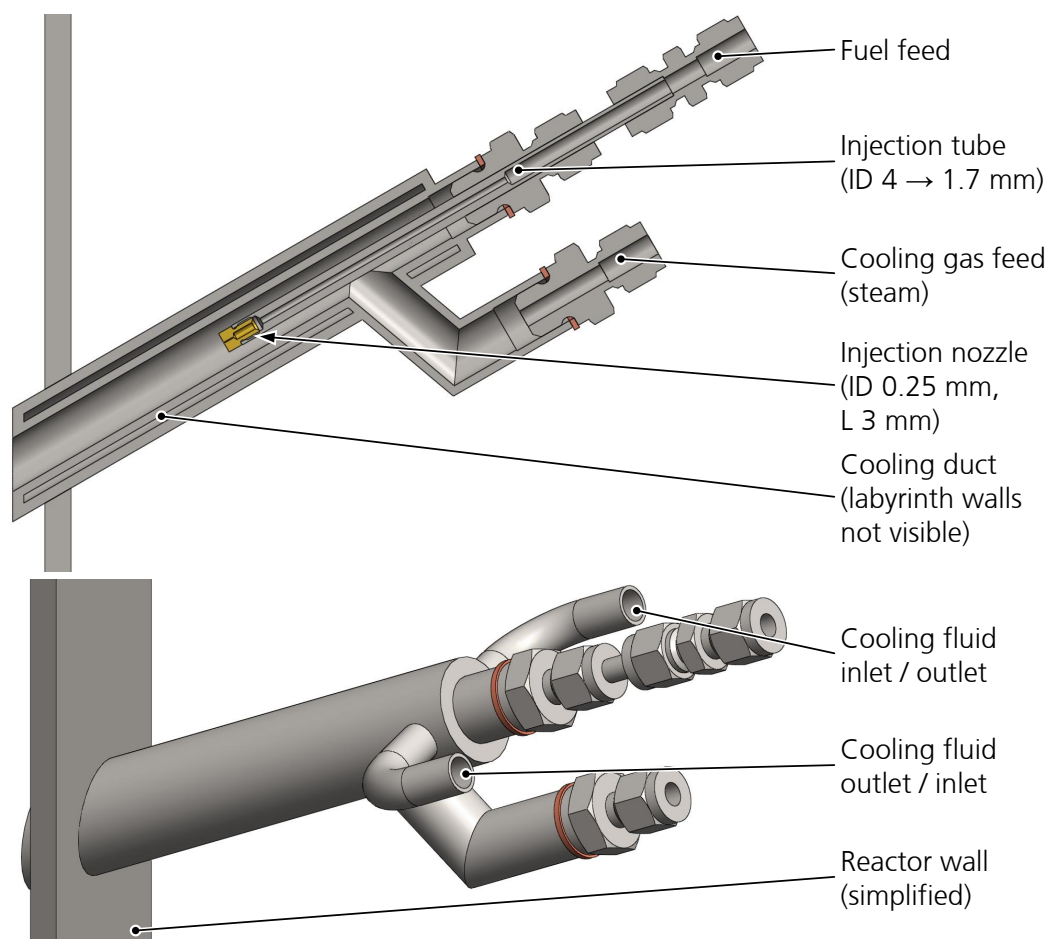


**Figure 3.9:** Different views of an improved fuel injection system for vacuum residue

Another measure that could possibly simplify the injection, while improving the distribution of liquid fuel in the fluidized bed, has been proposed by Lyngfelt et al. [87, 88]. The essential idea is to feed the fuel into a box. This box has a downward opening and is immersed in the fluidized bed of the fuel reactor. The oxygen-carrier particles will not enter the box, whereas gas from within the box will mix with the fluidized bed along the edges of the opening. The idea was proposed for solid fuels, which contain volatiles that are difficult to distribute in a fluidized bed. However, this concept seems very practical even for liquid fuels. Upon conversion, the volume of the fuel molecules increases significantly and the formation of large bubbles or gas channels is likely, which, in turn, deteriorates the contact between fuel and oxygen carrier. If such a fuel distributor would be employed, the fuel could be fed to the reactor close to the wall, which decreases heat transfer to the injection system, while possibly improving the distribution of fuel in the fluidized bed. Because of its simplicity, this kind of fuel distributor could be constructed in a small-scale reactor, like the pilot-scale reactor used here.



---

## 4 Conclusions

---

This thesis presents the first comprehensive investigation of chemical-looping combustion with liquid fuels. The work clearly shows that chemical-looping combustion with liquid fuels is technically feasible. The process was established in the bench-scale reactor with continuous injection of liquid fuel and a number of widely different oxygen-carriers, both synthetic and natural in origin. The process could be scaled up to a pilot-scale unit, which operates at conditions similar to those in an industrial circulating fluidized-bed boiler. In the pilot-scale unit, a fuel input of up to  $6 \text{ kW}_{\text{th}}$  was tested and a fuel blend was used that consisted to 80 wt% of vacuum residue. It was shown that fuel conversion does not change significantly for different types of liquid fuels. Fuel handling and injection, however, changed significantly and proved to be the main challenge during the scale-up process.

During the bench-scale experiments, several oxygen carriers clearly showed high reactivity and were able to convert the kerosene to  $\text{CO}_2$  and  $\text{H}_2\text{O}$  to a high extent. Especially copper-based materials had a high propensity to reach complete gas yield with very little unconverted species remaining in the flue gas. However, many oxygen carriers showed problems with respect to stability and mechanical integrity. One oxygen-carrier material, ilmenite, was identified to be potentially suitable for long-term operation, mainly due to its predicted long lifetime. Tests in a pilot-scale reactor were carried for more than 330 h in hot fluidized state, out of which 72 h were with addition of fuel. During that time, the oxygen carrier was very stable and did not show any signs of major chemical or structural degradation. Fuel conversion was not complete but could be improved by increasing the temperature, increasing the solid circulation or decreasing the fuel flow. A maximum gas yield of 88 mol% was achieved in this work. Another potentially feasible oxygen-carrier material, based on calcium manganite, was identified. Due to its oxygen release properties, fuel conversion was clearly higher than with ilmenite oxygen carrier.

Fuel conversion during experiments with 80 wt% vacuum residue and 20 wt% fuel oil 1 did not deviate in any significant way from experiments with fuel oil 1. Consequently, it is believed that unblended vacuum residue will have a conversion behaviour, which is similar to that of the fuel blends tested.



---

# Nomenclature

---

## Latin symbols

$f_{C,AR}$	(mol%)	carbon fraction fuel carbon that leaks into the air reactor; Eq. (7), p. 44
$f_{CH_4}$	(mol%)	carbon fraction of CO in the fuel reactor; Eq. (3), p. 36
$f_{CHO}$	(mol%)	carbon fraction of $C_xH_yO_z$ , except $CH_4$ , in the fuel reactor; Eq. (4), p. 36
$f_{CO}$	(mol%)	carbon fraction of CO in the fuel reactor; Eq. (2), p. 36
$g$	(m/s <sup>2</sup> )	gravitational acceleration constant = 9.81 m/s <sup>2</sup>
$G'_s$	(kg/m <sup>2</sup> s)	circulation index (gross mass-flux of oxygen carrier); Eq. (5), p. 43
$\dot{n}_{C,fuel}$	(mol/s)	molar flow of elemental carbon in the fuel added
$\dot{n}_{CO_2,AR,out}$	(mol/s)	molar flow of carbon dioxide leaving the air reactor compensated for atmospheric CO <sub>2</sub> concentration ( $\approx 400$ ppm)
$\dot{n}_{O_2,AR,in}$	(mol/s)	molar flow of oxygen entering the air reactor
$\dot{n}_{O_2,AR,out}$	(mol/s)	molar flow of oxygen leaving the air reactor
$\dot{n}_{O_2,stoich}$	(mol/s)	stoichiometric molar flow of oxygen needed for the combustion of fuel
$u_0$	(m/s)	superficial gas velocity
$u_t$	(m/s)	terminal velocity based on average particle size

## Greek symbols

$\gamma_{CO_2}$	(mol%)	CO <sub>2</sub> yield; Eq. (1), p. 36
$\Delta h$	(m)	vertical height difference of pressure measurement $\Delta p$ in the middle section of the riser = 0.678 m
$\Delta p$	(Pa)	pressure difference measured in the middle section of the riser
$\eta_{fuel}$	(%)	degree of fuel oxidation; Eq. (6), p. 44

---

## Acronyms

AR	air reactor
BET	Brunauer-Emmett-Teller (particle surface area)
C2Z-1050	20 wt% CuO / 80 wt% ZrO <sub>2</sub> calcined at 1050°C
C4MA4T2-1000	40 wt% CuO / 40 wt% MgAl <sub>2</sub> O <sub>4</sub> / 20 wt% TiO <sub>2</sub> calcined at 1000°C
CLC	chemical-looping combustion
CLOU	chemical-looping with oxygen uncoupling
CLR	chemical-looping reforming
FID	flame ionization detector
FR	fuel reactor
GC	gas chromatograph
M4MZ-1200	40 wt% Mn <sub>3</sub> O <sub>4</sub> / 60 wt% MgO-ZrO <sub>2</sub> calcined at 1200°C
N4MZ-1400	40 wt% NiO / 60 wt% MgO-ZrO <sub>2</sub> calcined at 1400°C
OC	oxygen carrier
TGA	thermogravimetric analyser
SEM	scanning electron microscopy
XRD	X-ray powder diffractometry

---

# Bibliography

---

- [1] S. Arrhenius. On the Influence of Carbonic Acid in the Air upon the Temperature of the Ground. *Philosophical Magazine and Journal of Science*, 41:237–276, 1896.
- [2] IPCC. *Climate Change 2014: Impacts, Adaptation, and Vulnerability. Part A: Global and Sectoral Aspects. Contribution of Working Group II to the Fifth Assessment Report of the Intergovernmental Panel on Climate Change*. Cambridge University Press, Cambridge, UK and New York, NY, 2014.
- [3] IPCC. *Climate Change 2014: Impacts, Adaptation, and Vulnerability. Part B: Regional Aspects. Contribution of Working Group II to the Fifth Assessment Report of the Intergovernmental Panel on Climate Change*. Cambridge University Press, Cambridge, UK and New York, NY, 2014.
- [4] UNFCCC. *Kyoto Protocol*. United Nations Framework Convention on Climate Change, 1998.
- [5] J. G. Olivier, G. Janssens-Maenhout, M. Muntean, and J. A. Peters. Trends in Global CO<sub>2</sub> Emissions: 2013 report. Technical report, PBL Netherlands Environmental Assessment Agency, The Hague, The Netherlands, 2013.
- [6] UNFCCC. Decisions adopted by the conference of the parties. In *Report of the Conference of the Parties on its sixteenth session, held in Cancun from 29 November to 10 December 2010*. United Nations Framework Convention on Climate Change, 2011.
- [7] M. Meinshausen, N. Meinshausen, W. Hare, S. Raper, K. Frieler, R. Knutti, D. Frame, and M. Allen. Greenhouse-gas emission targets for limiting global warming to 2°C. *Nature*, 458(7242):1158–1162, 2009.
- [8] J. Rogelj, D. McCollum, A. Reisinger, M. Meinshausen, and K. Riahi. Probabilistic cost estimates for climate change mitigation. *Nature*, 493(7430):79–83, 2013.
- [9] IPCC. *Climate Change 2014: Mitigation of Climate Change. Contribution of Working Group III to the Fifth Assessment Report of the Intergovernmental Panel on Climate Change*. Cambridge University Press, Cambridge, UK and New York, NY, 2014.
- [10] IPCC. *IPCC Special Report on Carbon Dioxide Capture and Storage*. Cambridge University Press, Cambridge, UK and New York, NY, 2005.

- [11] W. Lewis, E. Gilliland, and M. Sweeney. Gasification of Carbon — Metal Oxides in a Fluidized Powder Bed. *Chemical Engineering Progress*, 47(5):251–256, 1951.
- [12] M. Ishida and J. Hongguang. A novel combustor based on chemical-looping reactions and its reaction kinetics. *Journal of Chemical Engineering of Japan*, 27(3):296–301, 1994.
- [13] A. Lyngfelt and H. Thunman. Construction and 100 h of operational experience of a 10-kW chemical looping combustor. In *Carbon Dioxide Capture for Storage in Deep Geologic Formations - Results from the CO<sub>2</sub> Capture Project*, volume 1 – Capture and Separation of Carbon Dioxide From Combustion Sources, pages 625–646. Elsevier Science, Amsterdam, The Netherlands, 1<sup>st</sup> edition, 2005.
- [14] N. Berguerand and A. Lyngfelt. Design and operation of a 10 kW<sub>th</sub> chemical-looping combustor for solid fuels – Testing with South African coal. *Fuel*, 87:2713–2726, 2008.
- [15] P. Moldenhauer, M. Rydén, T. Mattisson, and A. Lyngfelt. Chemical-looping combustion and chemical-looping reforming of kerosene in a circulating fluidized-bed 300 W laboratory reactor. *International Journal of Greenhouse Gas Control*, 9:1–9, 2012.
- [16] L.-S. Fan. *Chemical Looping Systems for Fossil Energy Conversions*. John Wiley & Sons, Hoboken, NJ, 1<sup>st</sup> edition, 2010.
- [17] J. Adánez, A. Abad, F. García-Labiano, P. Gayán, and L. F. de Diego. Progress in chemical-looping combustion and reforming technologies. *Progress in Energy and Combustion Science*, 38(2):215–282, 2012.
- [18] A. Lyngfelt. Oxygen Carriers for Chemical-Looping Combustion. In *Calcium and chemical looping technology for power generation and carbon dioxide (CO<sub>2</sub>) capture*. Woodhead Publishing, 2014. accepted for publication.
- [19] A. Lyngfelt. Chemical-looping combustion of solid fuels – status of development. *Applied Energy*, 113:1869–1873, 2014.
- [20] M. Rydén, H. Leion, T. Mattisson, and A. Lyngfelt. Combined oxides as oxygen-carrier material for chemical-looping with oxygen uncoupling. *Applied Energy*, 113:1924–1932, 2014.
- [21] T. Mattisson, A. Lyngfelt, and H. Leion. Chemical-looping with oxygen uncoupling for combustion of solid fuels. *International Journal of Greenhouse Gas Control*, 3(1):11–19, 2009.
- [22] T. Mattisson, E. Jerndal, C. Linderholm, and A. Lyngfelt. Reactivity of a spray-dried NiO/NiAl<sub>2</sub>O<sub>4</sub> oxygen carrier for chemical-looping combustion. *Chemical Engineering Science*, 66(20):4636–4644, 2011.
- [23] M. Rydén, A. Lyngfelt, and T. Mattisson. Synthesis gas generation by chemical-looping reforming in a continuously operating laboratory reactor. *Fuel*, 85(12-13):1631–1641, 2006.

- 
- [24] M. Rydén, A. Lyngfelt, and T. Mattisson. Chemical-looping combustion and chemical-looping reforming in a circulating fluidized-bed reactor using Ni-based oxygen carriers. *Energy & Fuels*, 22:2585–2597, 2008.
- [25] J. Wolf, M. Anheden, and J. Yan. Performance of Power Generation Processes with Chemical Looping Combustion for CO<sub>2</sub> removal – Requirements for the Oxidation and Reduction Reactors. In *Proceedings of the 18th Annual International Pittsburgh Coal Conference*, Newcastle, Australia, 2001.
- [26] Ø. Brandvoll and O. Bolland. Inherent CO<sub>2</sub> capture using chemical looping combustion in a natural gas fired power cycle. *Journal of Engineering for Gas Turbines and Power*, 126(2):316–321, 2004.
- [27] IEA. Statistics — World: Electricity and Heat. online, 2014. URL <http://www.iea.org/statistics/>. [accessed: September 27, 2014].
- [28] IEA. Key World Energy Statistics. Technical report, International Energy Agency, 2014.
- [29] A. Forret, A. Hoteit, and T. Gauthier. Chemical Looping Combustion Process applied to liquid fuels. In *British–French Flame Days*, pages 37–38, Lille, France, 2009.
- [30] A. Hoteit, A. Forret, W. Pelletant, J. Roesler, and T. Gauthier. Chemical Looping Combustion with Different Types of Liquid Fuels. *Oil and Gas Science and Technology*, 66(2):193–199, 2011.
- [31] Y. Cao, B. Lia, H.-Y. Zhao, C.-W. Lin, S. P. Sit, and W.-P. Pan. Investigation of Asphalt (Bitumen)-fuelled Chemical Looping Combustion using Durable Copper-based Oxygen Carrier. *Energy Procedia*, 4:457–464, 2011.
- [32] J. Bao, W. Liu, J. Cleeton, S. Scott, J. Dennis, Z. Li, and N. Cai. Interaction between Fe-based oxygen carriers and n-heptane during chemical looping combustion. *Proceedings of the Combustion Institute*, 34(2):2839–2846, 2013.
- [33] P.-C. Chiu, Y. Ku, H.-C. Wu, Y.-L. Kuo, and Y.-H. Tseng. Spent isopropanol solution as possible liquid fuel for moving bed reactor in chemical looping combustion. *Energy & Fuels*, 28(1):657–665, 2014.
- [34] P. Moldenhauer, M. Rydén, T. Mattisson, and A. Lyngfelt. Chemical-looping combustion and chemical-looping with oxygen uncoupling of kerosene with Mn- and Cu-based oxygen carriers in a circulating fluidized-bed 300 W laboratory reactor. *Fuel Processing Technology*, 104:378–389, 2012.
- [35] P. Moldenhauer, M. Rydén, T. Mattisson, M. Younes, and A. Lyngfelt. The use of ilmenite as oxygen carrier with kerosene in a 300 W CLC laboratory reactor with continuous circulation. *Applied Energy*, 113:1846–1854, 2014.
- [36] P. Moldenhauer, M. Rydén, T. Mattisson, A. Hoteit, A. Jamal, and A. Lyngfelt. Chemical-Looping Combustion with Fuel Oil in a 10 kW Pilot Plant. *Energy & Fuels*, 28(9):5978–5987, 2014.

- [37] A. Serrano, F. García-Labiano, L. F. De Diego, P. Gayán, A. Abad, and J. Adánez. Ethanol combustion in a CLC unit using Ni- and Cu-based oxygen carriers. In *Proceedings of the 3rd International Conference on Chemical Looping*, Gothenburg, Sweden, 2014.
- [38] P. Pimenidou, G. Rickett, V. Dupont, and M. Twigg. Chemical looping reforming of waste cooking oil in packed bed reactor. *Bioresource Technology*, 101(16):6389–6397, 2010.
- [39] P. Pimenidou, G. Rickett, V. Dupont, and M. Twigg. High purity H<sub>2</sub> by sorption-enhanced chemical looping reforming of waste cooking oil in a packed bed reactor. *Bioresource Technology*, 101(23):9279–9286, 2010.
- [40] A. Lea-Langton, N. Giannakeas, G. Rickett, V. Dupont, and M. Twigg. Waste lubricating oil as a source of hydrogen fuel using chemical looping steam reforming. *SAE International Journal of Fuels and Lubricants*, 3(2):810–818, 2010.
- [41] A. Lea-Langton, R. M. Zin, V. Dupont, and M. V. Twigg. Biomass pyrolysis oils for hydrogen production using chemical looping reforming. *International Journal of Hydrogen Energy*, 37(2):2037–2043, 2012.
- [42] N. Giannakeas, A. Lea-Langton, V. Dupont, and M. V. Twigg. Hydrogen from Scrap Tyre Oil via Steam Reforming and Chemical Looping in a Packed Bed Reactor. *Applied Catalysis B: Environmental*, 126:249–257, 2012.
- [43] T. Mendiara, J. M. Johansen, R. Utrilla, P. Geraldo, A. D. Jensen, and P. Glarborg. Evaluation of different oxygen carriers for biomass tar reforming (I): Carbon deposition in experiments with toluene. *Fuel*, 90(3):1049–1060, 2011.
- [44] I. Iliuta and M. Iliuta. Biosyngas production in an integrated aqueous-phase glycerol reforming/chemical looping combustion process. *Industrial and Engineering Chemistry Research*, 52(46):16142–16161, 2013.
- [45] W. Wang. Thermodynamic and experimental aspects on chemical looping reforming of ethanol for hydrogen production using a Cu-based oxygen carrier. *International Journal of Energy Research*, 38(9):1192–1200, 2014.
- [46] H. Zhang, R. Xiao, M. Song, D. Shen, and J. Liu. Hydrogen production from bio-oil by chemical looping reforming: Characteristics of the synthesized metal organic frameworks for CO<sub>2</sub> removal. *Journal of Thermal Analysis and Calorimetry*, 115(2): 1921–1927, 2014.
- [47] E. García-Díez, L. F. De Diego, F. García-Labiano, A. Abad, P. Gayán, J. Adánez, and J. Ruiz. Chemical Looping Reforming of Ethanol in a 1 kW<sub>th</sub> Unit. In *Proceedings of the 3rd International Conference on Chemical Looping*, Gothenburg, Sweden, 2014.
- [48] M. Rydén, M. Johansson, E. Cleverstam, A. Lyngfelt, and T. Mattisson. Ilmenite with addition of NiO as oxygen carrier for chemical-looping combustion. *Fuel*, 89(11): 3523–3533, 2010.

- 
- [49] P. Moldenhauer, M. Rydén, and A. Lyngfelt. Testing of minerals and industrial by-products as oxygen carriers for chemical-looping combustion in a circulating fluidized-bed 300 W laboratory reactor. *Fuel*, 93:351–363, 2012.
- [50] A. Lyngfelt, B. Leckner, and T. Mattisson. A fluidized-bed combustion process with inherent CO<sub>2</sub> separation; application of chemical-looping combustion. *Chemical Engineering Science*, 56:3101–3113, 2001.
- [51] T. Olsen. An Oil Refinery Walk-Through. *Chemical Engineering Progress*, 110(5):34–40, 2014.
- [52] American Bureau of Shipping. Notes on Heavy Fuel Oil. Technical report, American Bureau of Shipping, Houston, TX, 1984.
- [53] A. Watkinson. Critical review of organic fluid fouling. Technical report, Argonne National Laboratory, Argonne, IL, 1988.
- [54] W. Shu. A Viscosity Correlation for Mixtures of Heavy Oil, Bitumen, and Petroleum Fractions. *Society of Petroleum Engineers Journal*, 24(3):277–282, 1984.
- [55] M. Rydén, M. Johansson, A. Lyngfelt, and T. Mattisson. NiO supported on Mg-ZrO<sub>2</sub> as oxygen carrier for chemical-looping combustion and chemical-looping reforming. *Energy & Environmental Science*, 2(9):970–981, 2009.
- [56] T. Mattisson, M. Johansson, and A. Lyngfelt. The use of NiO as an oxygen carrier in chemical-looping combustion. *Fuel*, 85(5-6):736–747, 2006.
- [57] F. García-Labiano, L. F. de Diego, P. Gayán, J. Adánez, A. Abad, and C. Dueso. Effect of Fuel Gas Composition in Chemical-Looping Combustion with Ni-Based Oxygen Carriers. 1. Fate of Sulfur. *Industrial and Engineering Chemistry Research*, 48(5):2499–2508, 2009.
- [58] L. Shen, Z. Gao, J. Wu, and J. Xiao. Sulfur behavior in chemical looping combustion with NiO/Al<sub>2</sub>O<sub>3</sub> oxygen carrier. *Combustion and Flame*, 157(5):853–863, 2010.
- [59] J. Adánez, A. Cuadrat, A. Abad, P. Gayán, L. F. de Diego, and F. García-Labiano. Ilmenite activation during consecutive redox cycles in chemical-looping combustion. *Energy & Fuels*, 24(2):1402–1413, 2010.
- [60] A. Cuadrat, A. Abad, L. De Diego, F. García-Labiano, P. Gayán, and J. Adánez. Prompt considerations on the design of Chemical-Looping Combustion of coal from experimental tests. *Fuel*, 97:219–232, 2012.
- [61] N. Berguerand and A. Lyngfelt. Operation in a 10 kW<sub>th</sub> chemical-looping combustor for solid fuel – Testing with a Mexican petroleum coke. *Energy Procedia*, 1(1):407–414, 2009.
- [62] E. Jerndal, H. Leion, L. Axelsson, T. Ekvall, M. Hedberg, K. Johansson, M. Källén, R. Svensson, T. Mattisson, and A. Lyngfelt. Using low-cost iron-based materials as oxygen carriers for chemical looping combustion. *Oil and Gas Science and Technology*, 66(2):235–248, 2011.

- [63] C. Linderholm, A. Lyngfelt, A. Cuadrat, and E. Jerndal. Chemical-looping combustion of solid fuels – Operation in a 10 kW unit with two fuels, above-bed and in-bed fuel feed and two oxygen carriers, manganese ore and ilmenite. *Fuel*, 102:808–822, 2012.
- [64] A. Cuadrat, A. Abad, P. Gayán, L. De Diego, F. García-Labiano, and J. Adánez. Theoretical approach on the CLC performance with solid fuels: Optimizing the solids inventory. *Fuel*, 97:536–551, 2012.
- [65] H. Leion, A. Lyngfelt, M. Johansson, E. Jerndal, and T. Mattisson. The use of ilmenite as an oxygen carrier in chemical-looping combustion. *Chemical Engineering Research and Design*, 86:1017–1026, 2008.
- [66] H. Leion, T. Mattisson, and A. Lyngfelt. Use of Ores and Industrial Products As Oxygen Carriers in Chemical-Looping Combustion. *Energy & Fuels*, 23:2307–2315, 2009.
- [67] M. Johansson, T. Mattisson, and A. Lyngfelt. Investigation of  $Mn_3O_4$  with stabilized  $ZrO_2$  for chemical-looping combustion. *Chemical Engineering Research and Design*, 84(9):807–818, 2006.
- [68] A. Abad, T. Mattisson, A. Lyngfelt, and M. Rydén. Chemical-looping combustion in a 300 W continuously operating reactor system using a manganese-based oxygen carrier. *Fuel*, 85(9):1174–1185, 2006.
- [69] P. Cho, T. Mattisson, and A. Lyngfelt. Comparison of iron-, nickel-, copper-, and manganese-based oxygen carriers for chemical-looping combustion. *Fuel*, 83(9):1215–1225, 2004.
- [70] M. Johansson. *Screening of oxygen-carrier particles based on iron-, manganese-, copper- and nickel oxides for use in chemical-looping technologies*. Phd thesis, Chalmers University of Technology, Gothenburg, Sweden, 2007.
- [71] T. Mattisson, H. Leion, and A. Lyngfelt. Chemical-looping with oxygen uncoupling using  $CuO/ZrO_2$  with petroleum coke. *Fuel*, 88(4):683–690, 2009.
- [72] C. Forero, P. Gayán, F. García-Labiano, L. F. de Diego, A. Abad, and J. Adánez. Effect of gas composition in Chemical-Looping Combustion with copper-based oxygen carriers: Fate of sulphur. *International Journal of Greenhouse Gas Control*, 4(5):762–770, 2010.
- [73] A. Abad, I. Adánez-Rubio, P. Gayán, F. García-Labiano, L. F. de Diego, and J. Adánez. Demonstration of chemical-looping with oxygen uncoupling (CLOU) process in a  $1.5 kW_{th}$  continuously operating unit using a Cu-based oxygen-carrier. *International Journal of Greenhouse Gas Control*, 6:189–200, 2012.
- [74] P. Gayán, I. Adánez-Rubio, A. Abad, L. F. de Diego, F. García-Labiano, and J. Adánez. Development of Cu-based oxygen carriers for Chemical-Looping with Oxygen Uncoupling (CLOU) process. *Fuel*, 96:226–238, 2012.

- 
- [75] I. Adánez-Rubio, M. Arjmand, H. Leion, P. Gayán, A. Abad, T. Mattisson, and A. Lyngfelt. Investigation of Combined Supports for Cu-Based Oxygen Carriers for Chemical-Looping with Oxygen Uncoupling (CLOU). *Energy and Fuels*, 27(7):3918–3927, 2013.
- [76] D. Jing, T. Mattisson, H. Leion, M. Rydén, and A. Lyngfelt. Examination of perovskite structure  $\text{CaMnO}_{3-\delta}$  with MgO addition as oxygen carrier for chemical looping with oxygen uncoupling using methane and syngas. *International Journal of Chemical Engineering*, 2013(No. 679560), 2013.
- [77] M. Källén, M. Rydén, C. Dueso, T. Mattisson, and A. Lyngfelt.  $\text{CaMn}_{0.9}\text{Mg}_{0.1}\text{O}_{3-\delta}$  as oxygen carrier in a gas-fired 10 kW<sub>th</sub> chemical-looping combustion unit. *Industrial and Engineering Chemistry Research*, 52(21):6923–6932, 2013.
- [78] P. Hallberg, M. Källén, D. Jing, F. Snijkers, J. van Noyen, M. Rydén, and A. Lyngfelt. Experimental investigation of  $\text{CaMnO}_{3-\delta}$  based oxygen carriers used in continuous Chemical-Looping Combustion. *International Journal of Chemical Engineering*, 2014 (No. 412517), 2014.
- [79] M. Rydén, P. Moldenhauer, S. Lindqvist, T. Mattisson, and A. Lyngfelt. Measuring attrition resistance of oxygen carrier particles for chemical looping combustion with a customized jet cup. *Powder Technology*, 256:75–86, 2014.
- [80] E. Jerndal, T. Mattisson, and A. Lyngfelt. Thermal analysis of chemical-looping combustion. *Chemical Engineering Research and Design*, 84(9):795–806, 2006.
- [81] M. Keller, M. Arjmand, H. Leion, and T. Mattisson. Interaction of mineral matter of coal with oxygen carriers in chemical-looping combustion (CLC). *Chemical Engineering Research and Design*, 92(9):1753–1770, 2014.
- [82] P. Markström, N. Berguerand, and A. Lyngfelt. The application of a multistage-bed model for residence-time analysis in chemical-looping combustion of solid fuel. *Chemical Engineering Science*, 65(18):5055–5066, 2010.
- [83] D. Kunii and O. Levenspiel. *Fluidization engineering*. Butterworth–Heinemann, Boston, MA, 2<sup>nd</sup> edition, 1991.
- [84] M. M. Azis, E. Jerndal, H. Leion, T. Mattisson, and A. Lyngfelt. On the evaluation of synthetic and natural ilmenite using syngas as fuel in chemical-looping combustion (CLC). *Chemical Engineering Research and Design*, 88(11):1505–1514, 2010.
- [85] A. Cuadrat, A. Abad, J. Adánez, L. De Diego, F. García-Labiano, and P. Gayán. Behavior of ilmenite as oxygen carrier in chemical-looping combustion. *Fuel Processing Technology*, 94(1):101–112, 2012.
- [86] M. Arjmand, R. Kooiman, M. Rydén, H. Leion, T. Mattisson, and A. Lyngfelt. Sulfur tolerance of  $\text{Ca}_x\text{Mn}_{1-y}\text{M}_y\text{O}_{3-\delta}$  (M = Mg, Ti) perovskite-type oxygen carriers in chemical-looping with oxygen uncoupling (CLOU). *Energy & Fuels*, 28(2):1312–1324, 2014.

- [87] A. Lyngfelt, D. Pallarès, C. Linderholm, M. Rydén, and T. Mattisson. Distributor of gases in the bottom part of a fluidized bed, 2014. Swedish patent application.
- [88] A. Lyngfelt. A 1000 MW<sub>th</sub> Chemical-Looping Combustor for solid fuels — discussion of design and costs. In *Proceedings of the 3rd International Conference on Chemical Looping*, Gothenburg, Sweden, 2014.